



NASA Langley Research Center

Multifunctional Nanocomposites for Aerospace Applications: Overview

CHEOL PARK

Advanced Materials and Processing Branch
NASA Langley Research Center
Hampton, VA 23681, USA

University of California, Merced
March 13, 2015



Acknowledgements



NASA Langley Research Center

Catharine Fay, Sharon Lowther, Wanda Gresham, Joseph Lee, Hoa Luong, Peter Gnoffo, Paul Danehy, Jennifer Inman, Steve Jones, Sheila Thibeault, Kristopher Wise, Andy Newman, Robert Bryant, Crystal Topping, Dennis Working, Keith Gordon, Sang Choi

National Institute of Aerospace

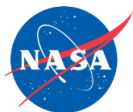
Vesselin Yamakov, Godfrey Sauti, Jin Ho Kang, Hyun Jung Kim, Sang-Hyon Chu, Luke Gibbons, Samantha Applin, Amanda Tiano

SUNY Binghamton

Meng Zheng, Xiaoming Chen, Changhong Ke, Howard Wang

Rice University

Mohammad Adnan, Matteo Pasquali



NASA C&I, B&P, GCD, IRAD, NIAC



NASA Langley Research Center



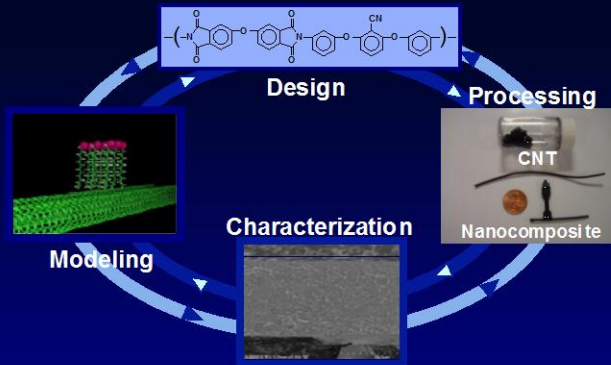
NASA Langley Research Center Hampton, Virginia
Founded in 1917: first civil aeronautical research laboratory
Facilities: \$4 billion replacement value
People: 2000 Civil Servants ; 1700 Contractors

All images credit: NASA

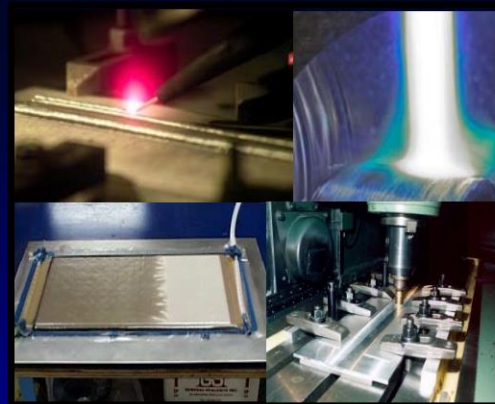
Advanced Materials and Processing Branch



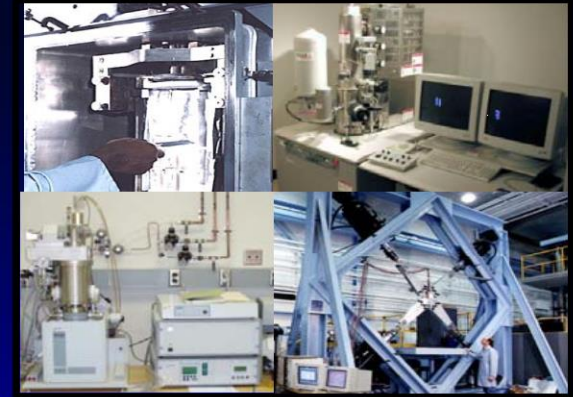
Materials Design



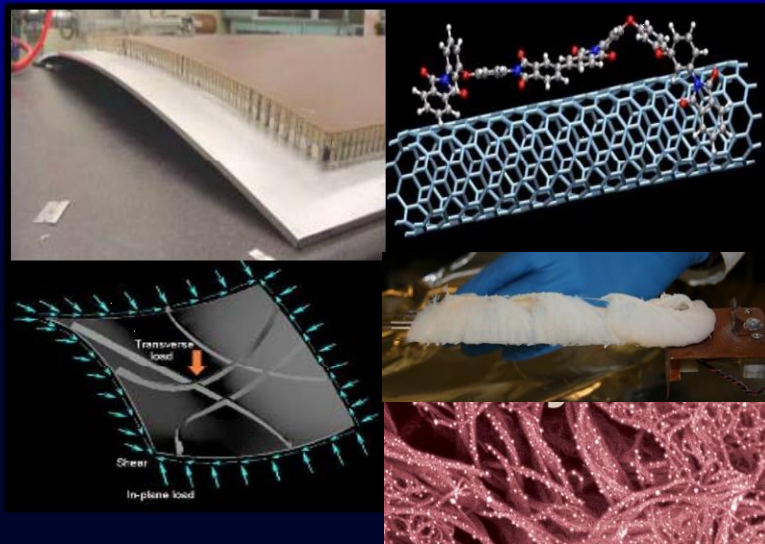
Innovative Materials Processing



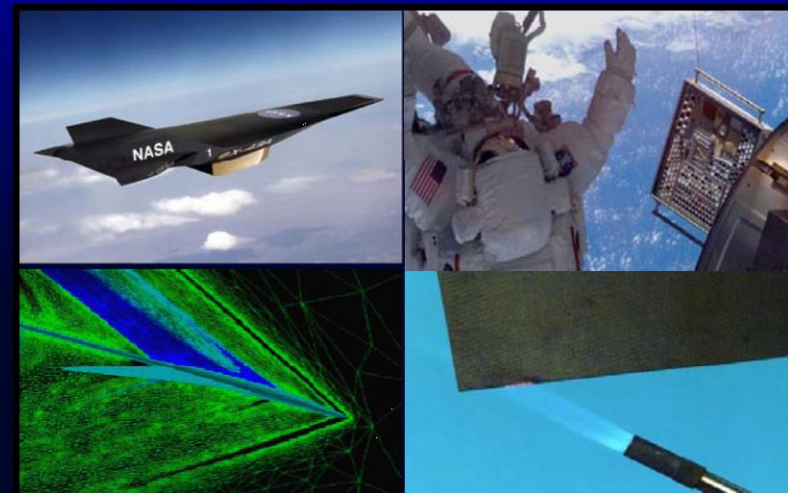
Materials Testing



Advanced Material Systems



Materials for Extreme Environments





Critical Concerns for Aerospace Systems

Weight

- Reduced fuel consumption & emissions
- Reduced launch costs
- Enabler for many new vehicles designs

Functionality/Performance

- Reduced fuel or power consumption
- Multifunctionality – additional reduced weight

Durability

- Safety and reliability
- Maintenance down-time and costs
- Extreme environments





Design Materials Properties

Materials Properties to be Tailored

- Electrical Conductivity
- Dielectric Permittivity
- Magnetic Permeability
- Thermal Conductivity/expansion coefficient
- Radiation Shielding
- Mechanical (modulus, strength, toughness...)
- Solar Absorptivity/Thermal Emissivity
- Band gap engineering
- Optical property (transparency, refractive index...)
- Piezoelectricity/Pyroelectricity/Electrostrictive
- Gas/Liquid Permeability
- Anisotropy/orientation

Design Parameters

- Nano Inclusion type and combination (CNT, BNNT, BCNNT, GP, hBN, NP...)
- Matrix type
- Composition
- Dispersion
- Orientation
- Geometry, Fabrication, Processing...

Specific Applications

- R2R Printing of Electroactive Polymer Composites: NSF/NASA
- Electroactive properties & Radiation Shielding of BNNT Composites: AFOSR/NASA C&I
- Radiation Detection and Conductivity Control: DOE (ORNL)/NASA
- Solar Absorption and Thermal Emission Control: NASA C&I
- Structural BNNT composites, BNNT fibers and mats: Rice Univ/NASA GCD, B&P, IRAD
- Multiple Metal Infusion for Multifunctionality (S2M2N): NASA IRAD
- Bandgap Engineering of nanotubes: NASA IRAD
- Doped Chiral Polymer Metamaterials (DCPM): NASA IRAD
- Radiation Shielding and Thermal Conduction (Electronic Packaging): NASA IRAD
- Ultralight Flexible Shielding Tension Shell: NASA IRAD

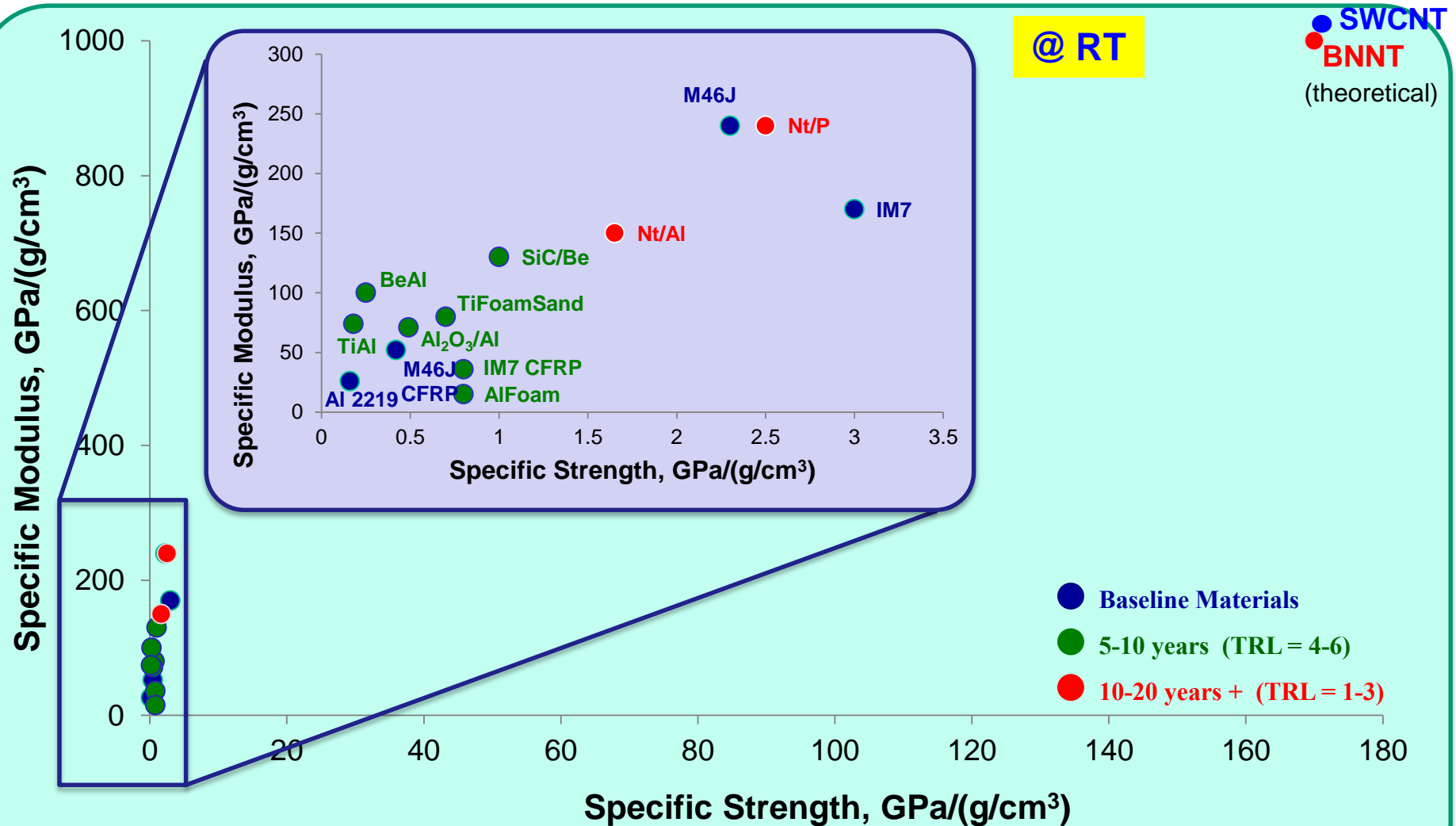


Outline

- Multifunctional Nanocomposites
 - Nanotube Synthesis: High Temperature-Pressure (HTP) BNNT and BCNNT Synthesis
 - Dispersion
 - Tailoring physical properties of nanocomposites for multifunctions
 - Metallized Nanotube Polymer Composites (MNPC)
 - Doped Chiral Polymer Metamaterials (DCPM)
 - Band Gap Engineering ($B_xC_yN_z$ Nanotubes)
- Sensors/Actuators
- Radiation Shielding
- Summary

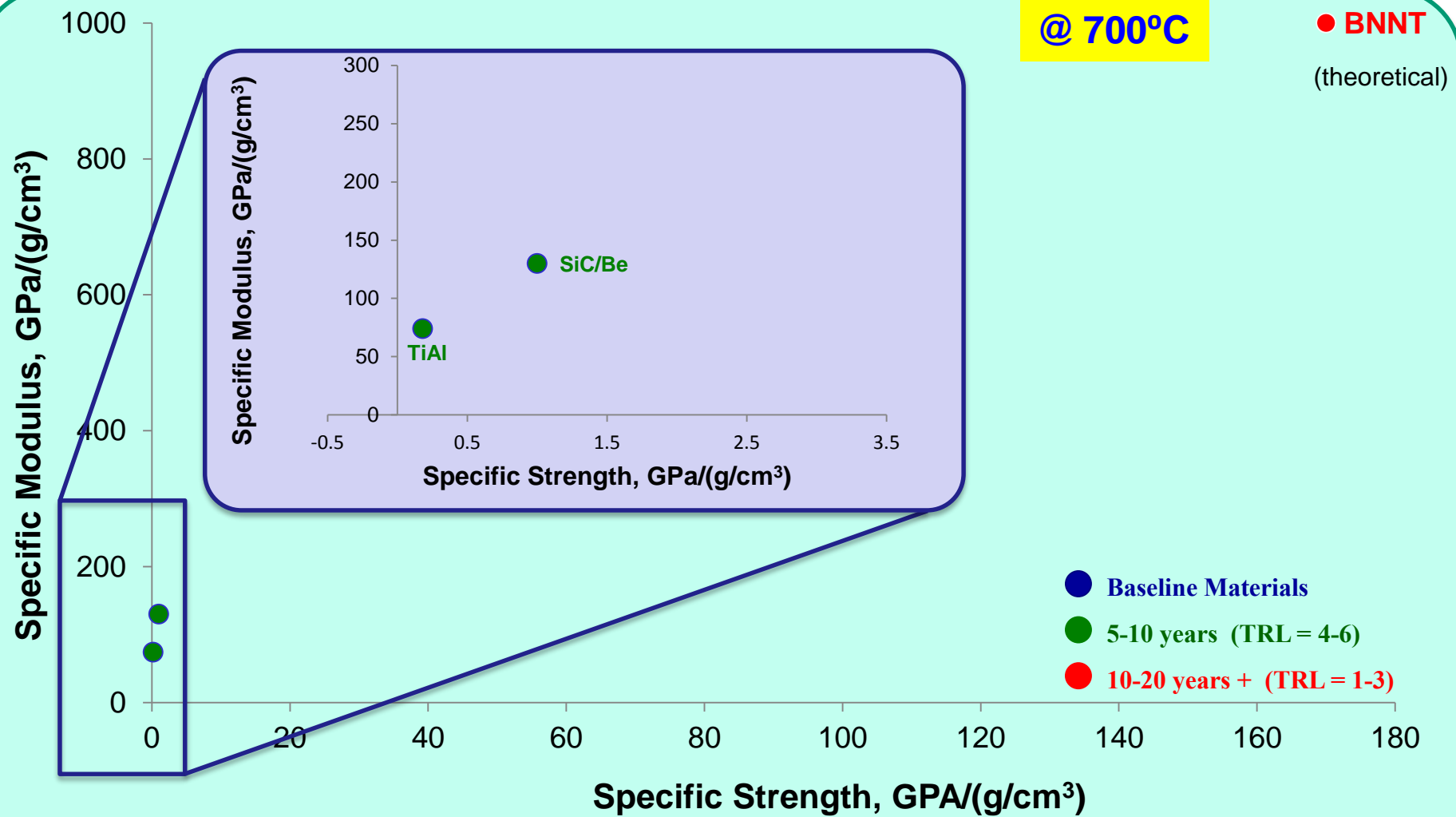


Properties of Materials for Vehicle Structure





Properties of Materials for Vehicle Structure





Nanotube Comparison (Theoretical)

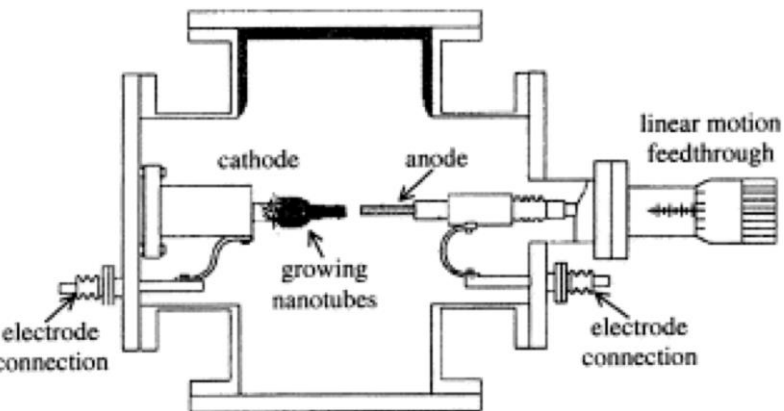


	Carbon Nanotubes	Boron Nitride Nanotubes
Electric Properties	Metallic or semiconducting	Wide band gap (about 6.0 eV band gap)
Mechanical Properties (Young's Modulus)	1.33 TPa (very stiff)	1.18 TPa (very stiff)
Thermal Conductivity	>3000 W/mK (highly conductive)	~300–3000 W/mK (highly conductive)
Thermal Oxidation Resistance	Stable up to 300-400 °C in air	Stable to over 800 °C in air
Neutron Absorption Cross-Section	C = 0.0035 barn	B = 767 barn (B ¹⁰ ~3800 barn) N = 1.9 barn (Excellent radiation shielding)
Polarity	No dipole	Permanent dipole Piezoelectric (0.25-0.4 C/m ²)
Surface Morphology	Smooth	Corrugated (Provides better bonding for composites, ionic bonding)
Color	Black	White (can be dyed to color)
Coefficient of Thermal Expansion	-1 x10 ⁻⁶ K ⁻¹ (very low)	-1 x 10 ⁻⁶ K ⁻¹ (very low)

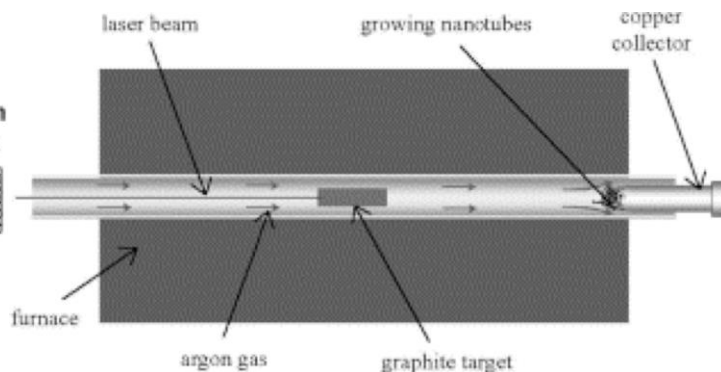


Synthesis Methods of Carbon Nanotubes

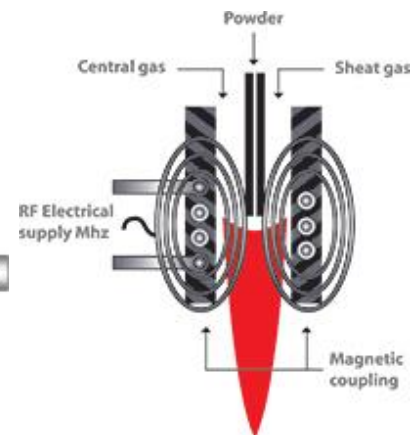
- Arc-discharge: solid state carbon precursor
- Laser ablation: solid state carbon precursor
- Chemical vapor deposition (CVD): gaseous carbon precursor/ HiPco (High pressure CO)
- Free Electron Laser (Jefferson Lab): funded by NASA-LaRC C&I
- RF Induction Thermal Plasma (Canadian NRC)



Arc-discharge

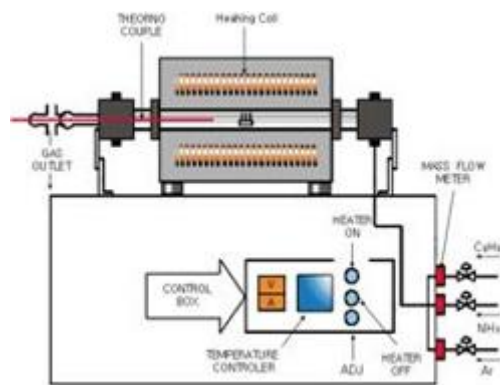


Laser ablation

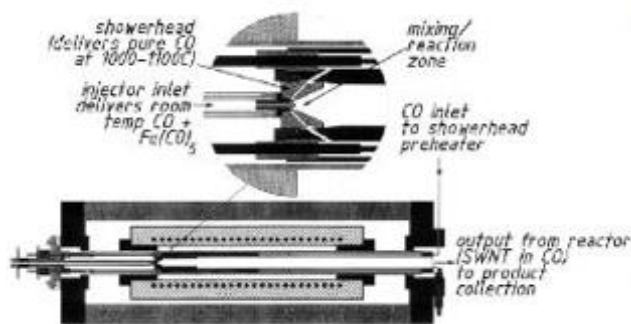


Credit: www.tekna.com

Induction Plasma



Chemical vapor deposition (CVD)



HiPco

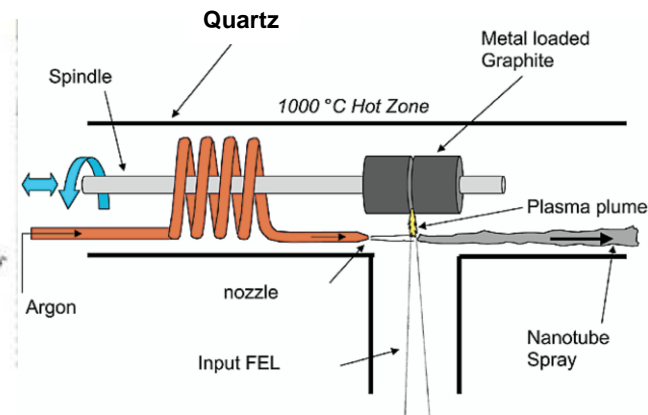


Image credit: NASA



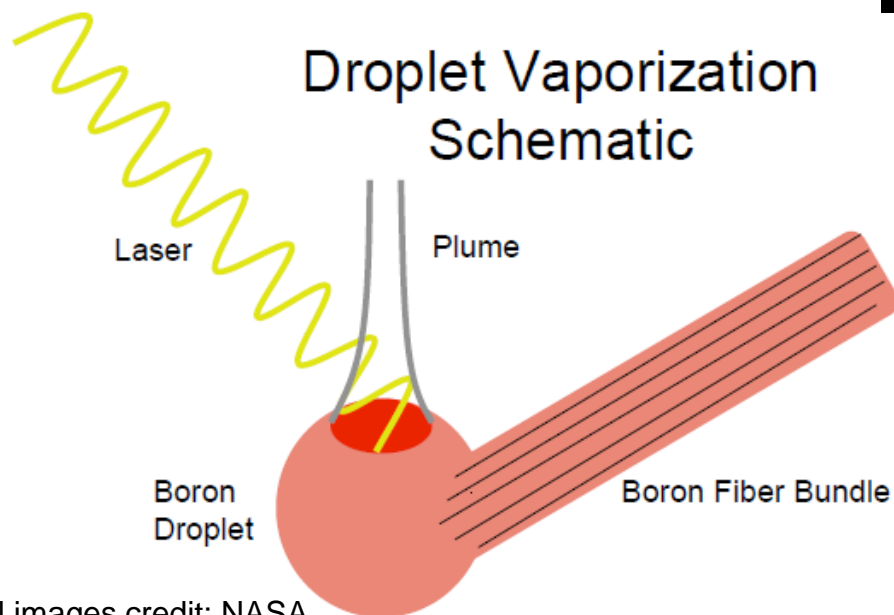
BNNT Synthesis History

- First Theoretical prediction: *PRB* **49** 5081–5084 (1994) (UC Berkeley, Cohen), computation
- First Synthesis Arc Discharge: *Science* **269** 966 (1995) (UC Berkeley, Cohen/Zettl) BNNT by Arc Discharge
- Arc Discharge: *PRL* **76** 4737 (1996) (ONERA France, Loiseau) Arc Discharge HfB₂ with N₂ gas
- Laser heating: *APL* **69** 2045 (1996) (NIMS Japan, Golberg, Bando), Diamond Anvil, c-BN target laser heating High pressure
- Laser ablation: *APL* **72** 1966 (1998) (Yu, BN powder with Co/Ni, first laser ablation
- Ball milling/thermal annealing: *CPL* **74** 2782 (1999) (ASU Australia, Chen) Ball milling of B powder in NH₃ gas
- CVD: *Chem. Mater.* **12** 1808 (2000) (WA Univ, Lourie, Ruoff, Buhro) CVD Borazine (B₃N₃H₆)
- Laser ablation, *PRB* **64** 121405(R) (2001) (ONERA Lee, Loiseau) CO₂ laser, no catalyst
- CVD: *Solid State Comm.* **135** 67 (2005) (NIMS, Zhi. Bando, Golberg) CVD NH₃ B₂O₃ from MgO/B powder
- High Temp, High Pressure, Laser vaporization: *Nanotechnology* **20** 505604 (2009) (NIA/NASA/Jlab) High Temperature, Pressure (HTP) BNNT, Free Electron Laser/CO₂ Laser
- High Temp Induction Thermal Plasma: *ACS Nano* **8** 6211 (2014) (NRC Canada, Kim, Kingston, Simard): 20g/hr, need H₂
- High Temp, High Press Induction Thermal Plasma: *NL* **14** 4881 (2014) (UC Berkeley, Zettl): 35g/hr



High Temperature-Pressure (HTP) BNNT and BCNNT

- Free Electron Laser or CO₂ laser
- No Catalyst, only B and N resource (and C for BCNNT)
- Very long, small diameter, highly crystalline BNNT, BCNNT



- 5 kW of infrared radiation @ $10.6\mu\text{m}$
- Heat source for vaporizing Boron feed stock above 3500°C
- Pressurized with Nitrogen to 200 psi
- LaRC rig operating since May 2012 daily with two operators for 1 shift

Nanotechnology, **20** 505604 (2009)
J. Thermophysics and Heat Transfer **27** 369 (2013)
Proc. SPIE **9060** 906006 (2014)

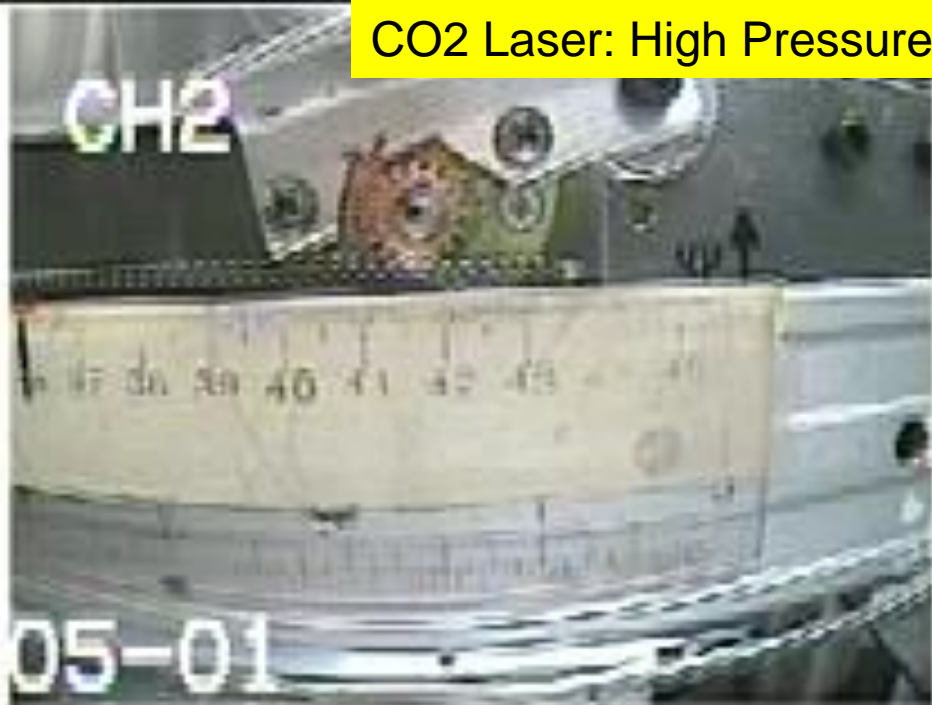


Free Electron Laser: Atmosphere: Spark



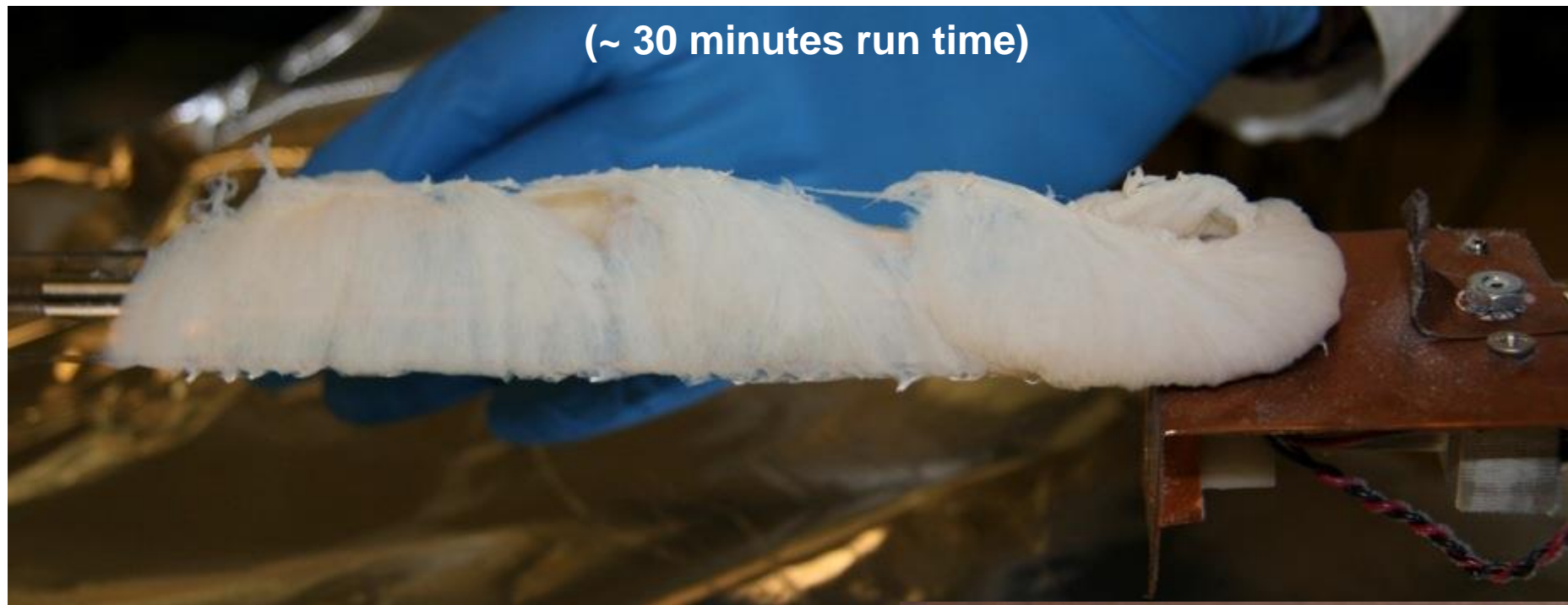
Free Electron Laser: High Pressure: BNNT Streamer







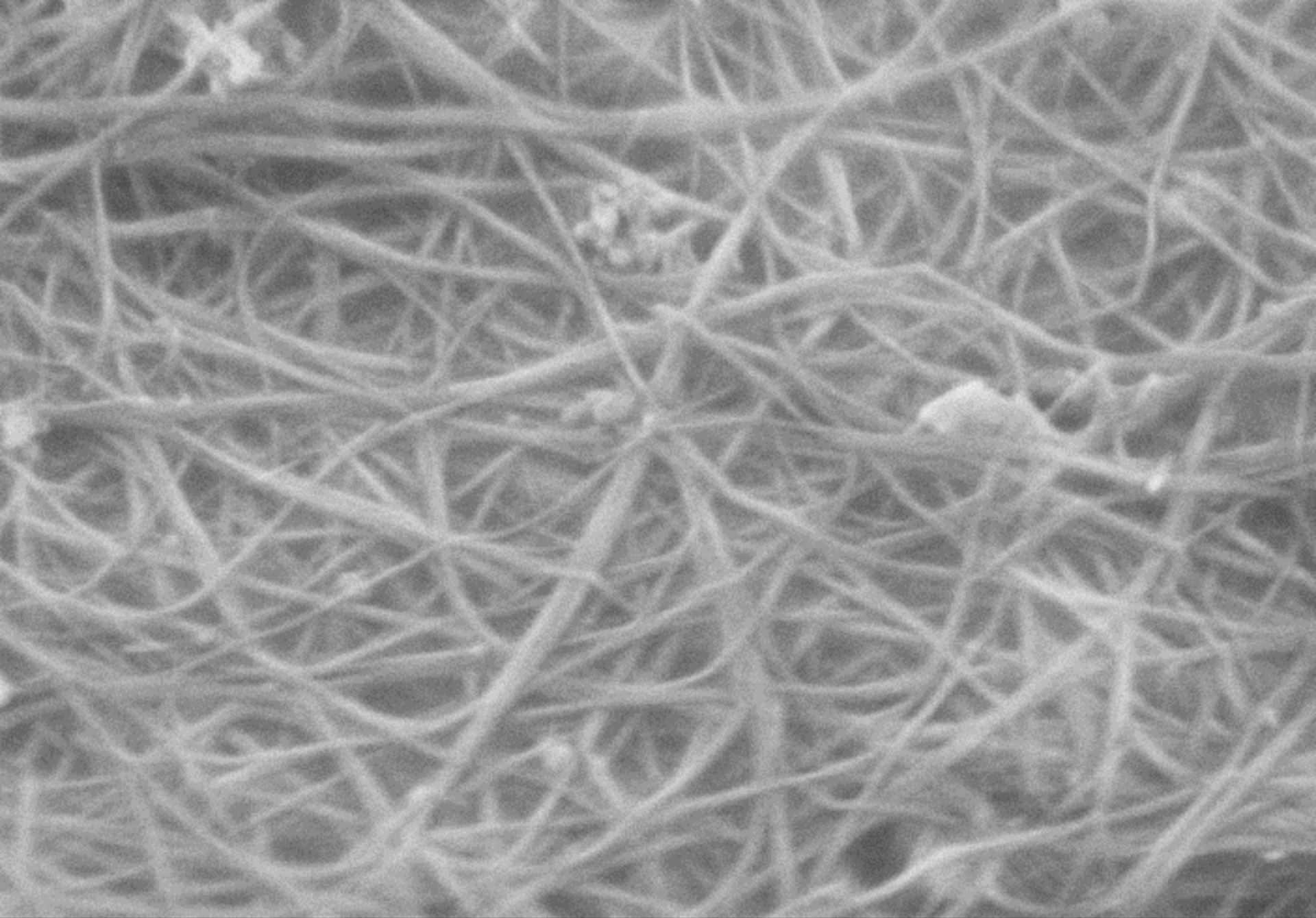
Cotton-like High Pressure and Temperature (HPT)-BNNT



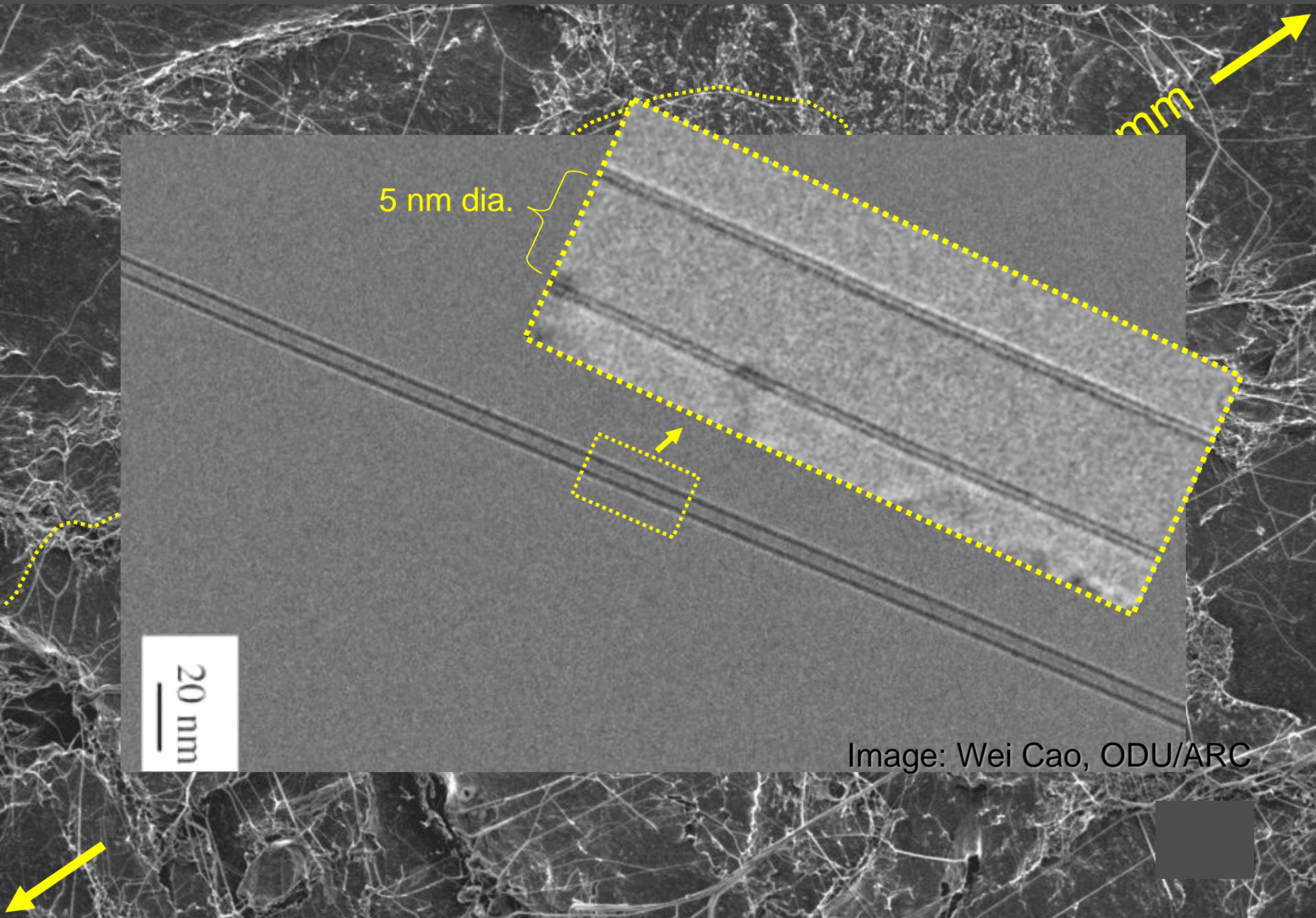
Benefits

- One-to-few-walled tubes with high crystallinity
- Very long, high-aspect ratio tubes
- High scale-up potential
- No toxic catalysts (only B and N as reactants)
- Standard industrial cutting/welding lasers
- High service temperature (over 800°C)
- Highly electroactive (due to the B-N polar bond)
- Neutron radiation shielding (due to their B content)





500nm



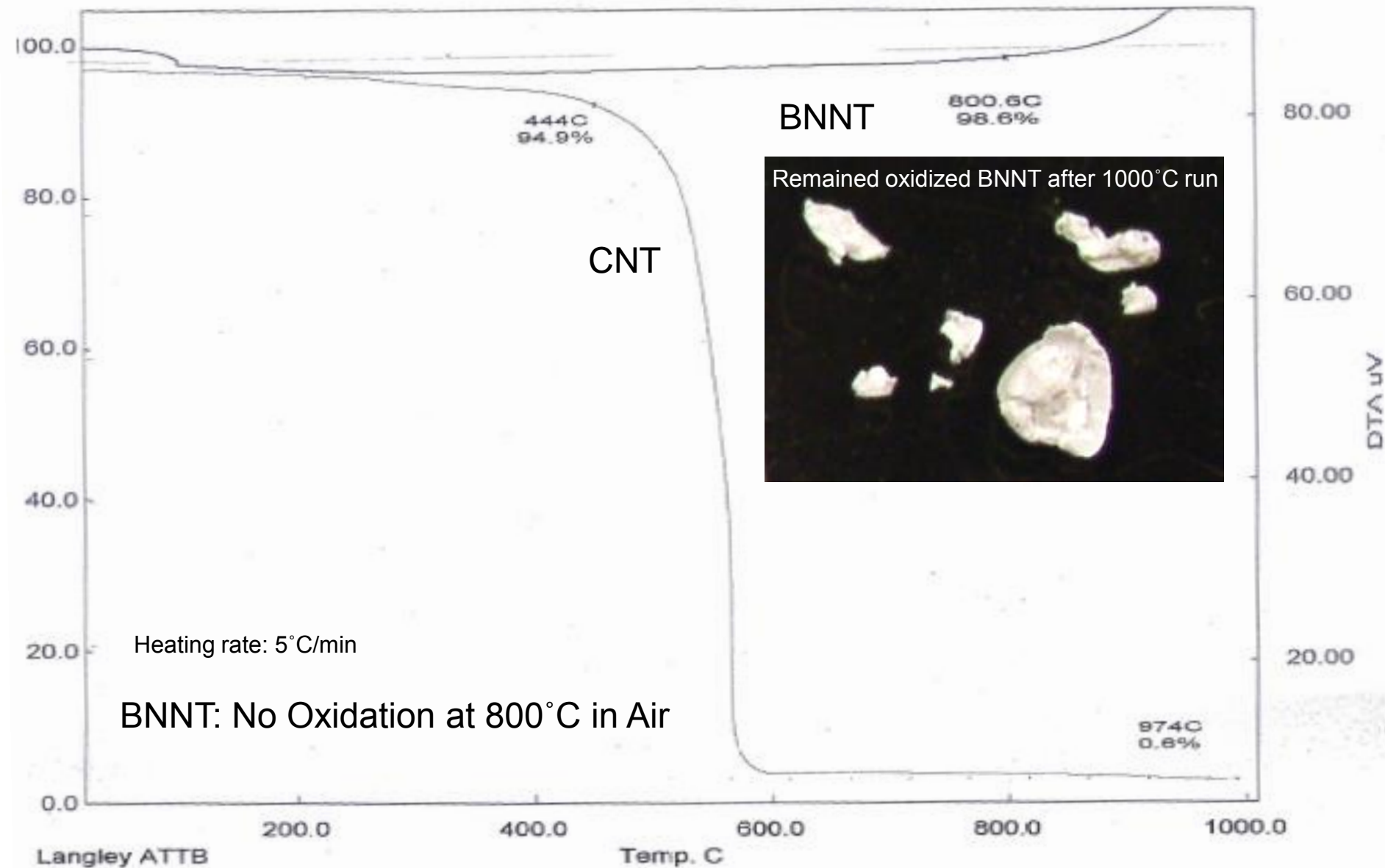
5 nm dia.

20 nm

Image: Wei Cao, ODU/ARC



Thermal Stability of BNNT vs. CNT: TGA





Mechanical Properties of BNNT and BNNT Composites: Processing and Characterization Techniques

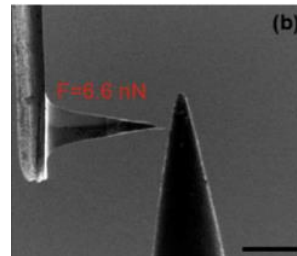
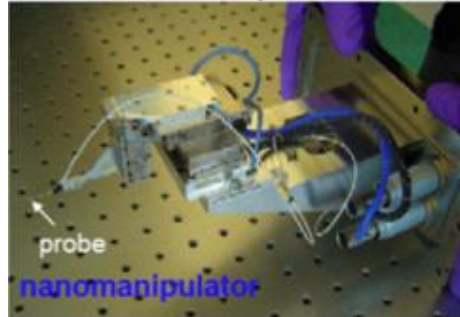
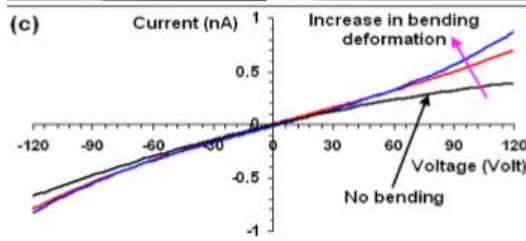
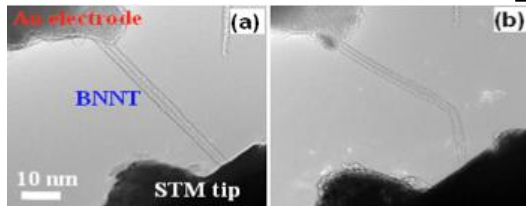
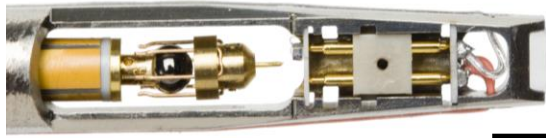
Individual BNNT and BNNT Bundles: compressive modulus, tensile modulus and strength, radial modulus

TEM-AFM, TEM-STM Holders

Credit: NASA LaRC/NIA/Binghamton

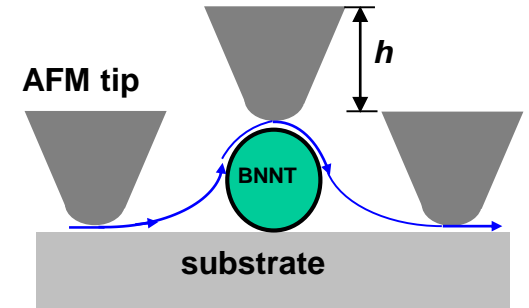
3D Nanomanipulator in SEM/FIB

Credit: SUNY Binghamton



AFM

Credit: SUNY Binghamton



Small, 8, 116 (2012)

ACS Nano, 6, 1814 (2012)

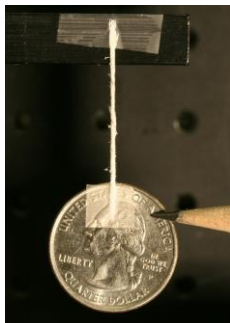
Nanotechnology, 23, 095703 (2012)

BNNT composites and BNNT yarns

Spun yarns: NASA LaRC/NIA (credit)

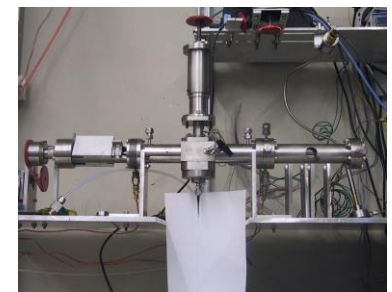
Wet spinning/Electrospinning

Credit: NASA LaRC/NIA



Superacid Spinning

Credit: Rice U



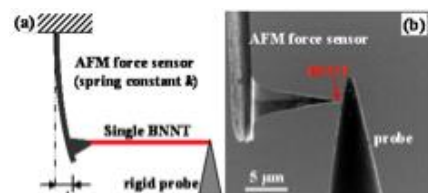
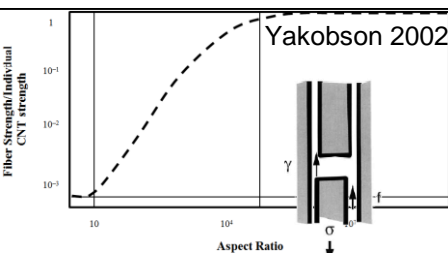


How to make strong, stiff, tough structural BNNT composite?

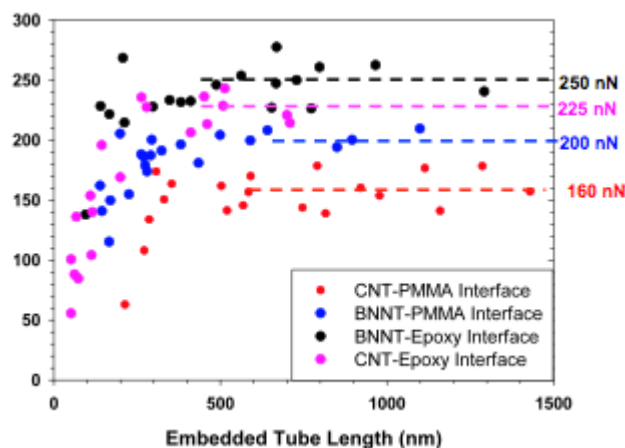
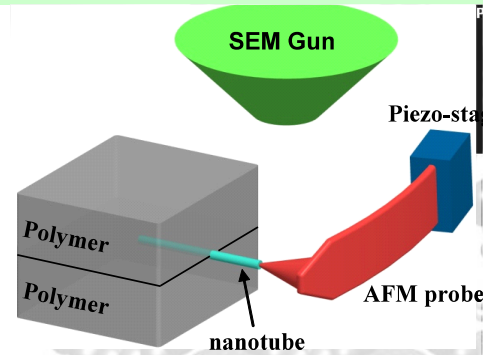
Good tubes:

highly crystalline,
long, thin BNNTs →
Excellent intrinsic
BNNT properties

Longer tube (high aspect ratio)
→ Greater yarn strength

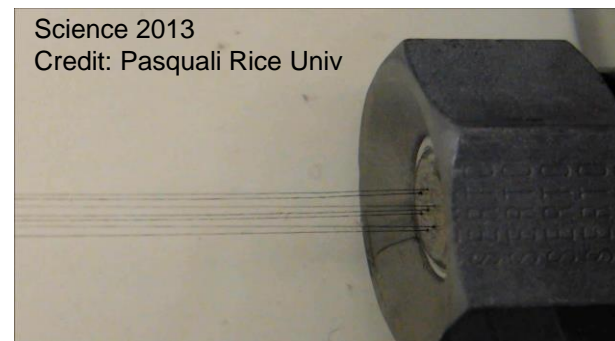


High interfacial strength



BNNT-epoxy and BNNT-PMMA interfacial strength are superior to CNT counterpart
(Small, 9, 3345 (2013))

High orientation



Hearle's Yarn Equation

$$\sigma_y \approx \cos^2 \zeta (1 - k \cos \zeta) \cdot \sigma_f$$

σ_y : yarn strength, σ_f : fiber (tube) strength
 ζ : helix angle that fibers make with yarn axis
 k : $(dQ/\mu)^{1/2}/3L$, d : fiber diameter
 μ : coefficient of friction, L : fiber length
 Q : fiber migration length

$$\text{If } \sigma_f \uparrow, d \downarrow, L \uparrow, \mu \uparrow \rightarrow \sigma_y \uparrow$$

BNNT Tensile Test Results (Only for comparison with CNT)

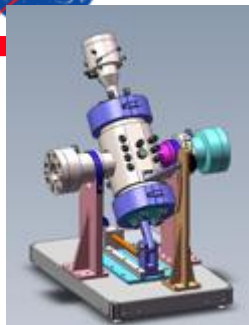
Diameter	Elastic modulus (GPa)	Breaking Strength (GPa)
D = 2.5 nm	760-960	14-38

Credit: Prof Ke (SUNY Binghamton)

Credit: Hearle, Structural mechanics of fibers, yarns, & fabrics, (1969)



NIA Research and Innovation Laboratories



NIA Lab Bldg



NIA BNNT Science Rig in a Safety Hutch



First BNNT run successfully without optimization
July 2013; excellent quality (long, thin, highly crystalline BNNT)

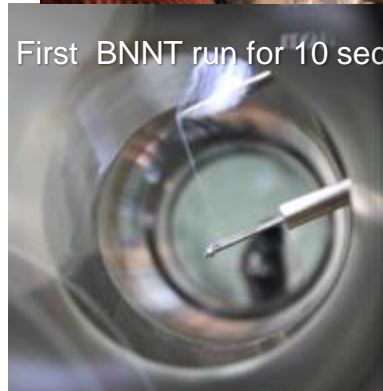
Successful pressure test up to **950 psi** (higher pressure leads to better BNNT potentially)

In-situ diagnostic tools installed (planar laser induced fluorescence: PLIF); more tools coming (CARS, pyrography, high speed camera...)

Parallel computational study for nucleation and growth ongoing (both NIA and NASA)

All images credit: NASA/NIA

First BNNT run for 10 sec



200 psi, 1kW

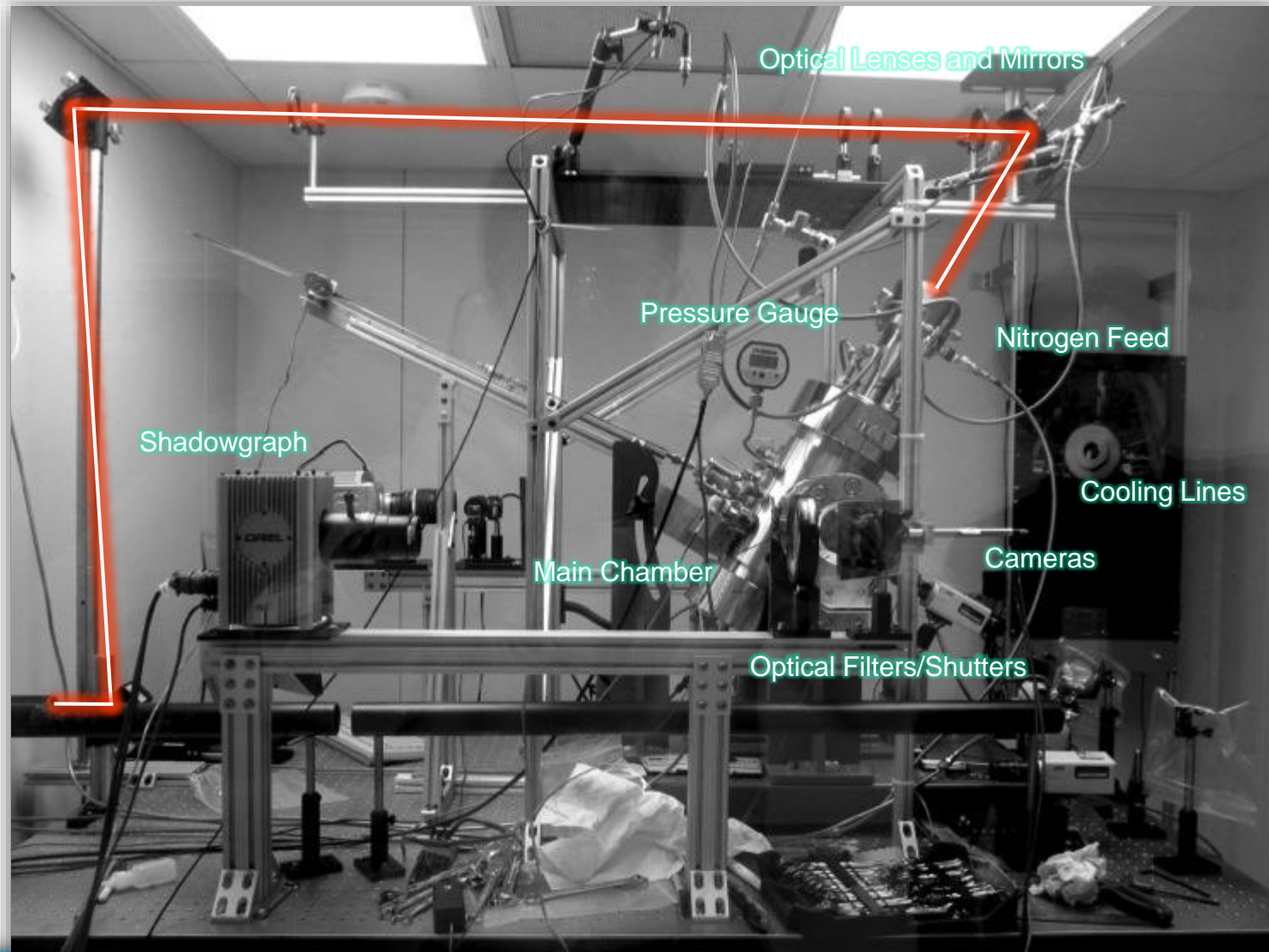


SWBNNT

Figure 3: TEM & SEM images: as grown BNNT

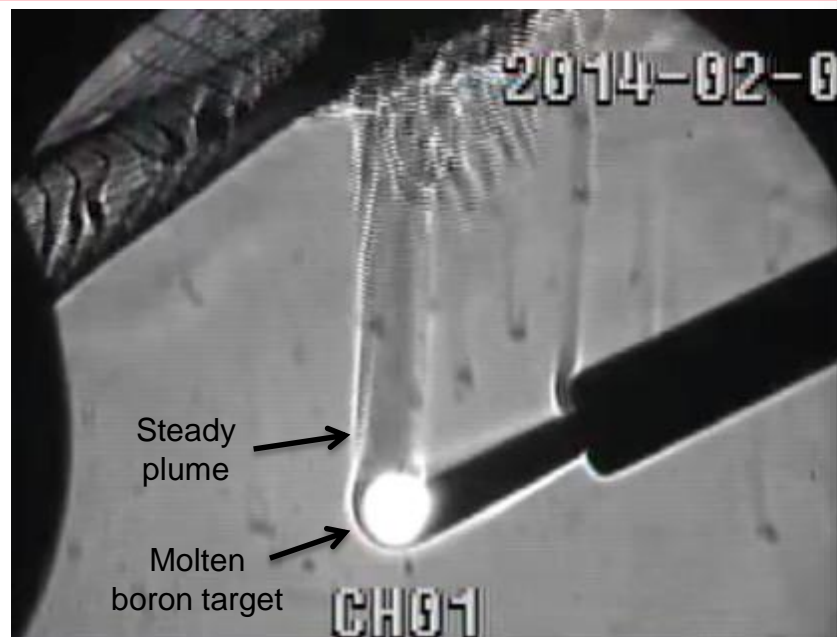


NIA BNNT Science Chamber

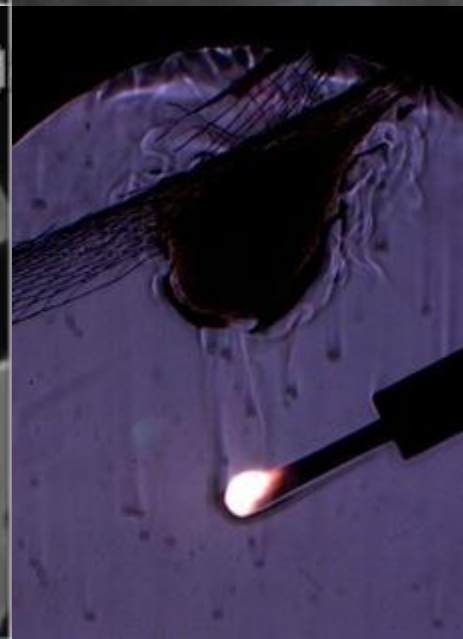




NIA Science Rig HTP BNNT Run (Snapshots)



All images credit: NASA/NIA

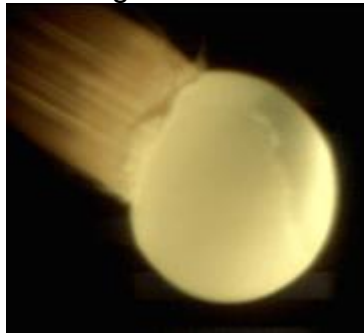




In-situ Optical Diagnostics

- ◆ Understand chemistry and flow physics of nanotube generation
- ◆ Improve and validate simulation/modeling
- ◆ Optimize material properties, production rate
- ◆ Specific Goals:
 - Determine gas and melt-ball temperatures
 - Determine amount of B_2 , B, BN, N and N_2
- ◆ In-situ, on-surface measurement:
 - High speed imaging; high speed (1 kHz) optical pyrometer being developed to study melt-ball dynamics
- ◆ Off-surface, gas phase measurement:
 - High-speed, high-resolution imaging
 - Shadowgraph and visible emission
 - Species sensitive imaging (BN PLIF)
 - Temperature measurements (CARS)

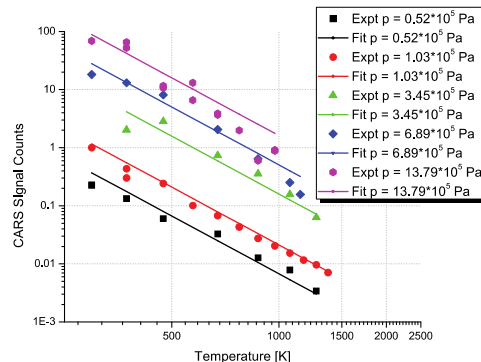
All images credit: NASA/NIA



High Speed Camera



Shadowgraph



CARS Intensity Measurement

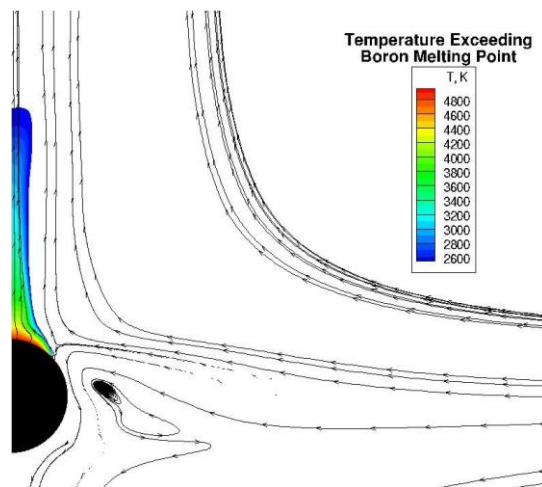


AIAA SciTech2014-1098 (2014)

Proc. SPIE **9060** 906006 (2014)



Modeling of Laser Ablation and Plume Chemistry in a Boron Nitride Nanotube Production Rig



Mass fraction of B, Plume Base

Pressurized Cylinder

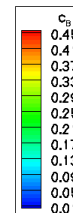
Radius = 5 cm

Height = 10 cm

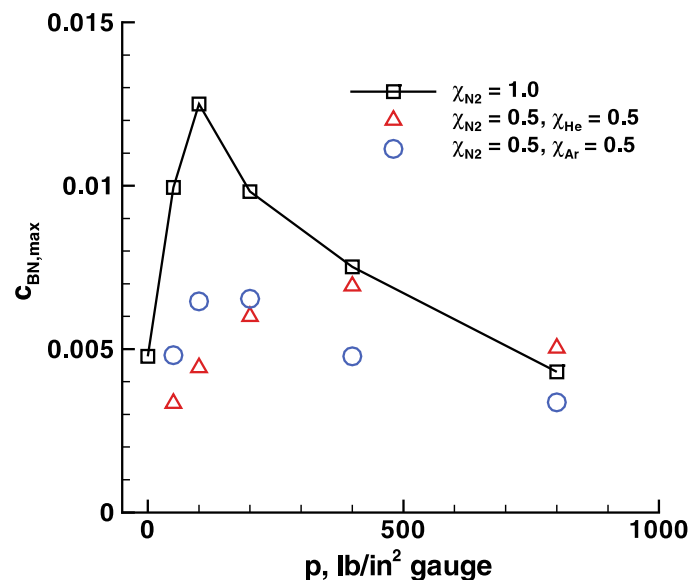
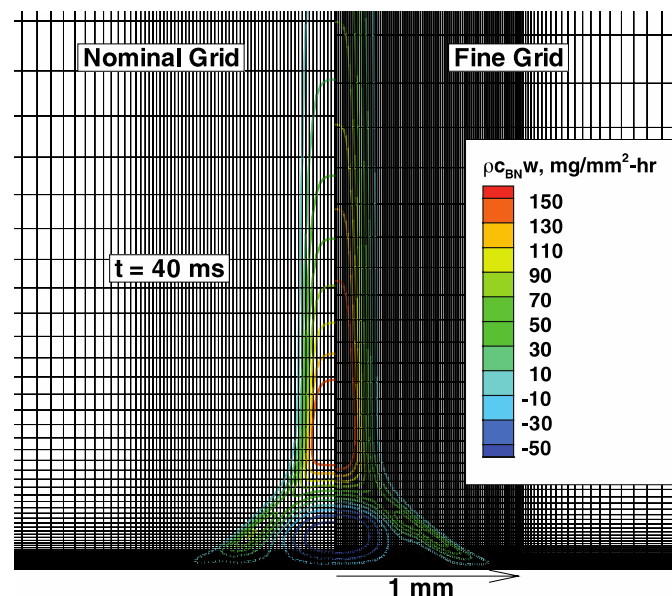
Vertical line on left is cylinder axis.
The second vertical line is offset 1 mm from axis.
The right boundary is a porous wall designed to maintain internal pressure.

Top and bottom boundaries - except for laser spot on bottom left - are fixed temperature, no-slip, equilibrium catalytic.

At time $t=0$ a laser delivers constant energy flux to the 1 mm radius spot on lower left, initiating vaporization of boron target and buoyancy driven plume to rise from hot spot.



Contour lines of temperatures and mass fraction of BN in the plume



All images credit: NASA

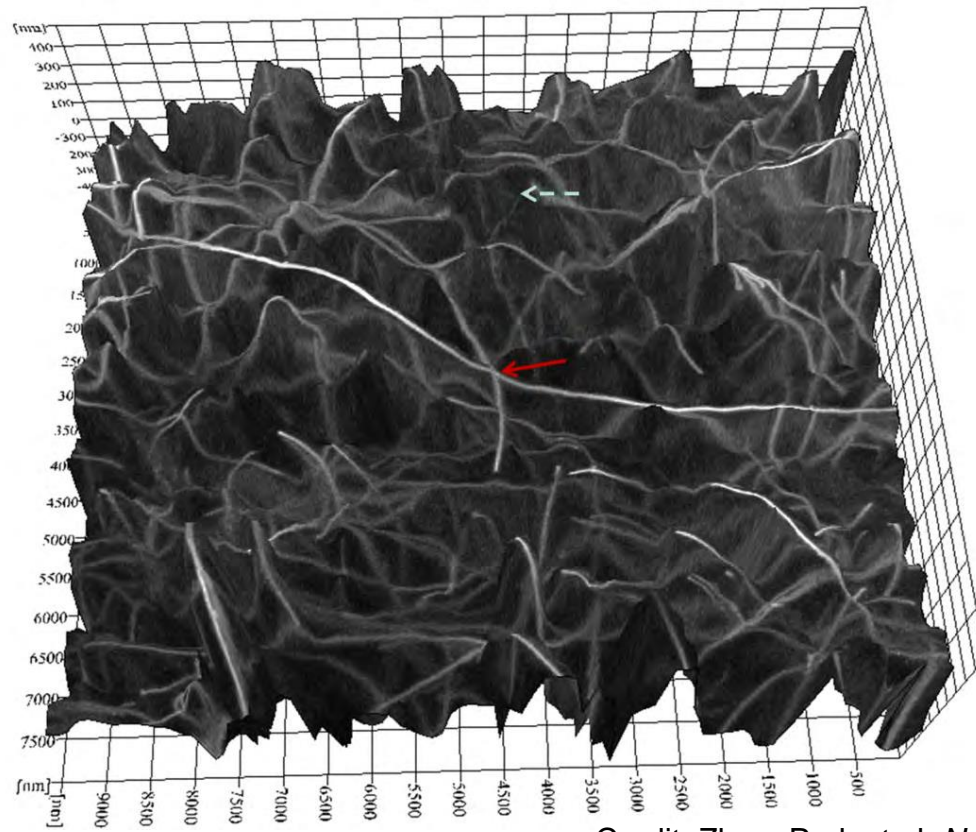
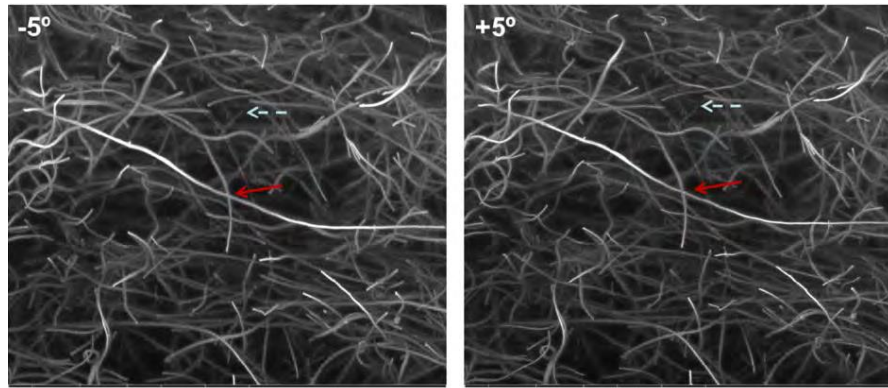
Fig. 5 Contour lines of BN flow rates in the plume.

a) Total chamber pressure

Proc. SPIE 9060 906006 (2014)

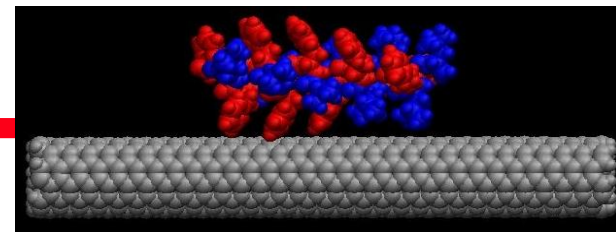
J. Thermophysics and Heat Transfer 27 369 (2013)

Dispersion





How to disperse Nanotubes?



1) Kinetic Approach

High shear (stirring, homogenization, speedmix)

Sonication (cavitation force)

Melt mixing (twin screw mixer, extruder, calendering, capillary rheometer, fiber spinning)

In-situ polymerization

In-situ polymerization under simultaneous sonication & high shear (Chem. Phys. Lett. 364, 303 (2002))

2) Thermodynamic Approach (Minimizing free energy of mixing)

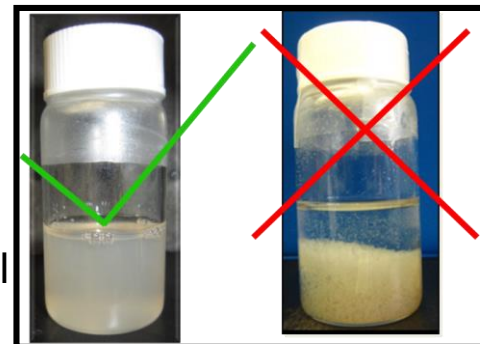
Covalent bonding

Acid etching

Stirring, reflux, and soxhlet extraction with H_2SO_4 , HNO_3 , and HCl

Functionalization

Fluorination, reflux with amine, electrochemical (diazonium compound)



Non-covalent bonding

Amphiphilic (surfactant), hydrophobic interaction: Water soluble polymers

Wrapping: PmPV, Polyvinyl pyrrolidone, Polystyrene sulfonate, PPE

Charge Transfer (Donor-acceptor) (Chem. Phys. Lett. 391, 207 (2004))

Dispersion Interaction (London force, Permittivity matching)

Solvent or Co-solvent selection (Hansen solubility parameter, surface energy)

Similar size/structure to SWCNT

Zwitterion

Complex formation

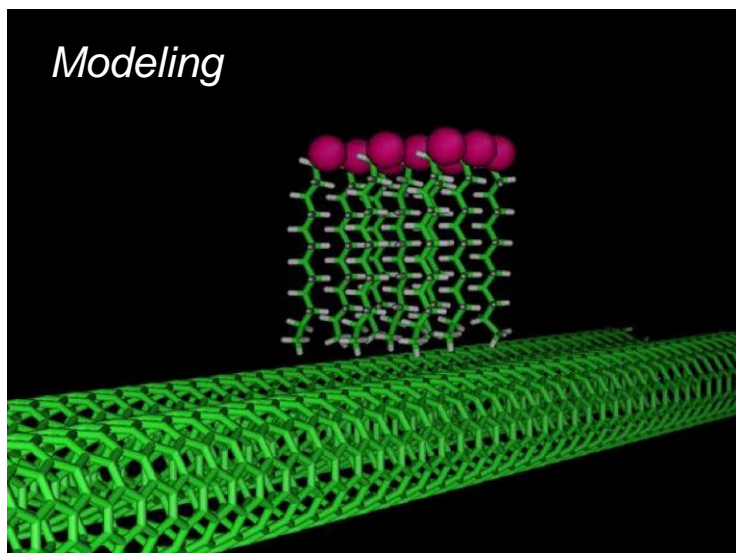
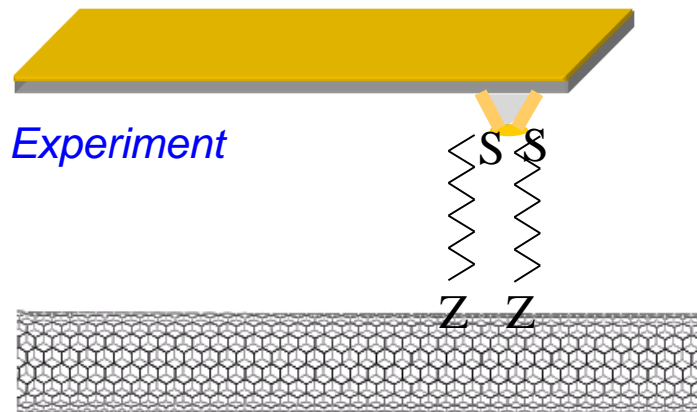
Nonspecific interaction

$$\Delta G_{\text{mix}} = \Delta H_{\text{mix}} - T^* \Delta S_{\text{mix}}$$



Adhesion Between Nanotubes & Various Functional Groups

- Using Functionalized AFM tips interaction forces can be directly probed.



Alkyl-thiol Endgroup	Experiment Force/Molecule (pN)	Modeling (pN)
–OH	9.6 ± 2	
–perfluoro	8.7 ± 3	
–SH	9.2 ± 3	
–CH=CH ₂	8.1 ± 2	
–CH ₃	7.6 ± 2	1.92
–COOH	12.2 ± 3	
–NH ₂	23.4 ± 4	2.98
Aryl-thiol Endgroup		
4-methylbenzene	18.9 ± 5.7	
4-nitrobenzene	21.8 ± 5.3	
4-aminebenzene	22.6 ± 4.7	
4-bromobenzene	26.9 ± 3.6	
4-hydroxybenzene	32.0 ± 8.4	
4-fluorobenzene	39.5 ± 8.8	
4-methoxybenzene	41.5 ± 10.9	
H-benzene	46.8 ± 11.8	
4-Nitrilebenzene	56.9 ± 15.5	



Hansen and Hilderbrand Solubility 3D Plot for BNNT

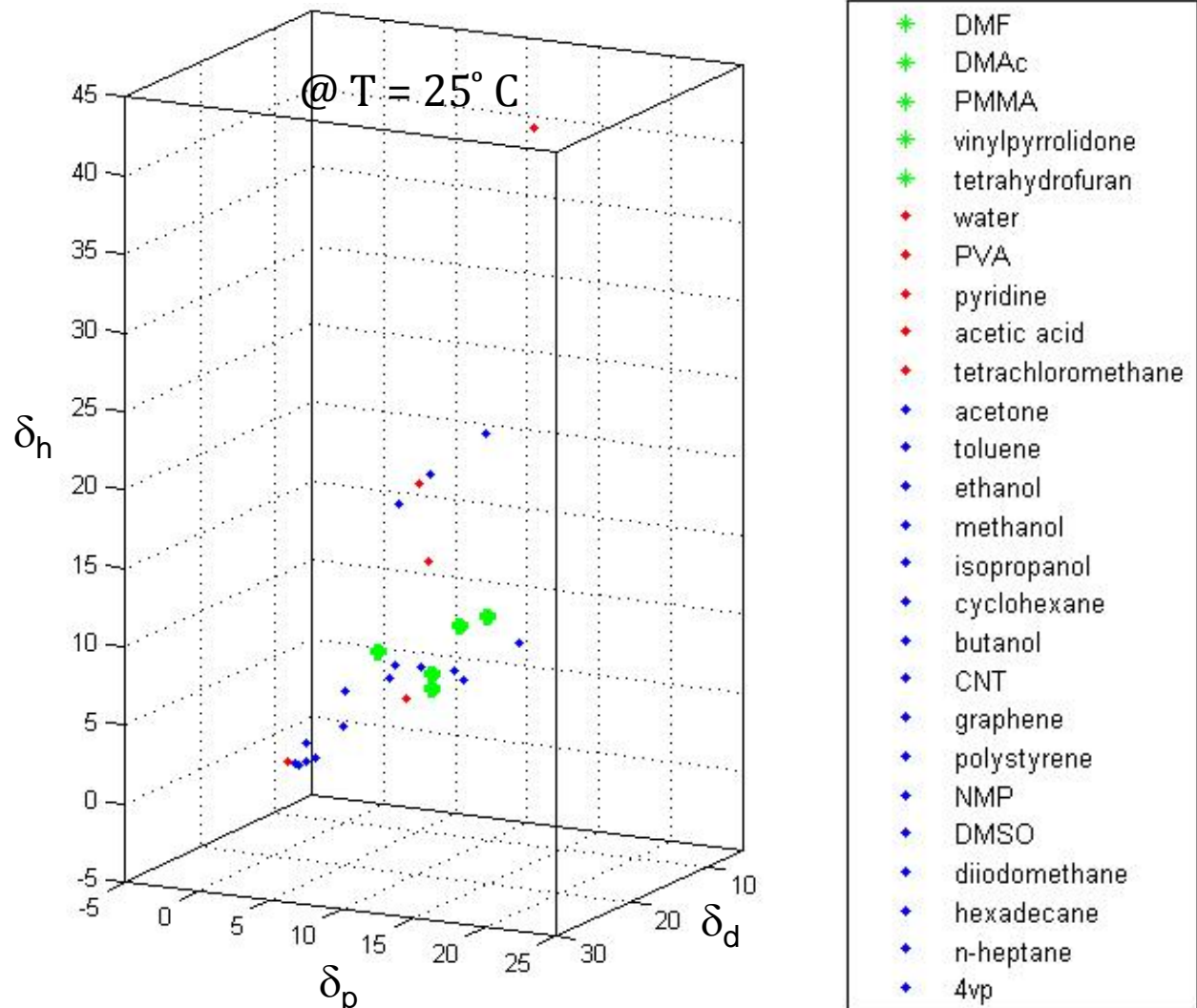
Hansen and Hildebrand Solubility: $d_t^2 = d_d^2 + d_p^2 + d_h^2$

δ_d : dispersion component

δ_p : polar

δ_h : hydrogen bond

Code written to plot coordinates (δ_d , δ_p , δ_h) for each solvent and color code good, poor, and unknown solvents

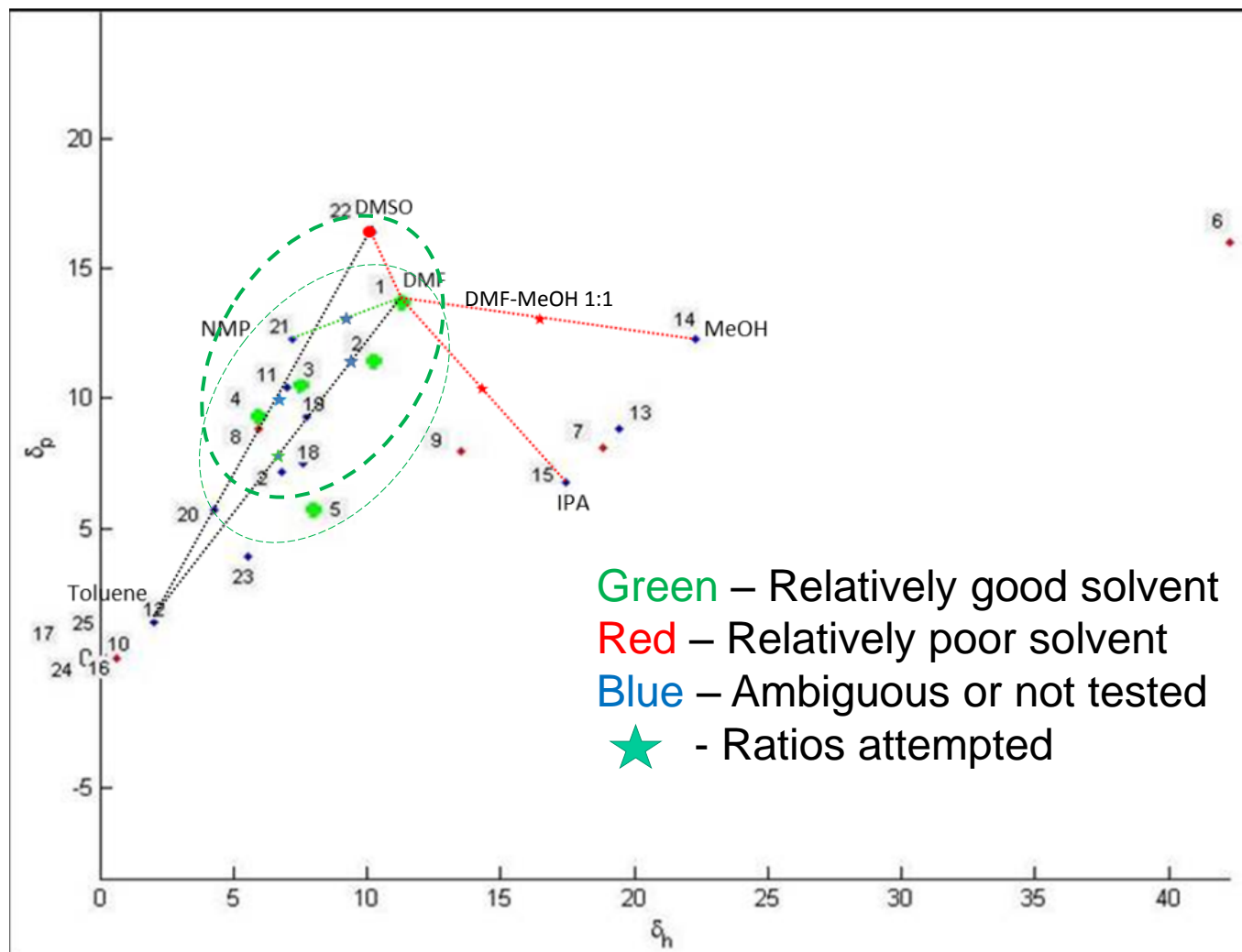




2-D Hansen Plot (δ_p , δ_h only): Select Good Solvents/Co-Solvents

Hansen and Hilderbrand Solubility:

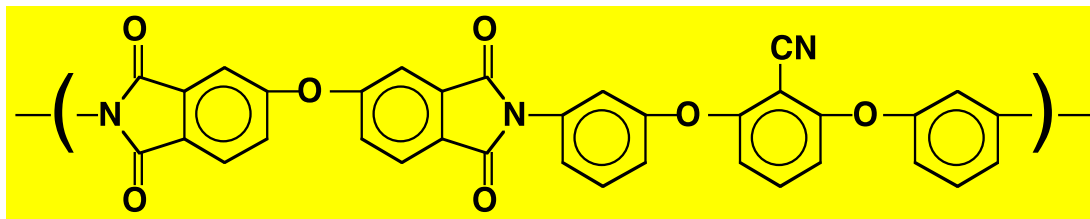
$$d_t^2 = d_d^2 + d_p^2 + d_h^2$$



- ★ 1) DMF
- ★ 2) DMAc
- ★ 3) PMMA
- ★ 4) vinylpyrrolidone
- ★ 5) tetrahydrofuran
- ◆ 6) water
- ◆ 7) PVA
- ◆ 8) pyridine
- ◆ 9) acetic acid
- ◆ 10) tetrachloromethane
- ◆ 11) acetone
- ◆ 12) toluene
- ◆ 13) ethanol
- ◆ 14) methanol
- ◆ 15) isopropanol
- ◆ 16) cyclohexane
- ◆ 17) butanol
- ◆ 18) CNT
- ◆ 19) graphene
- ◆ 20) polystyrene
- ◆ 21) NMP
- ◆ 22) DMSO
- ◆ 23) diiodomethane
- ◆ 24) hexadecane
- ◆ 25) n-heptane
- ◆ 26) 4vp

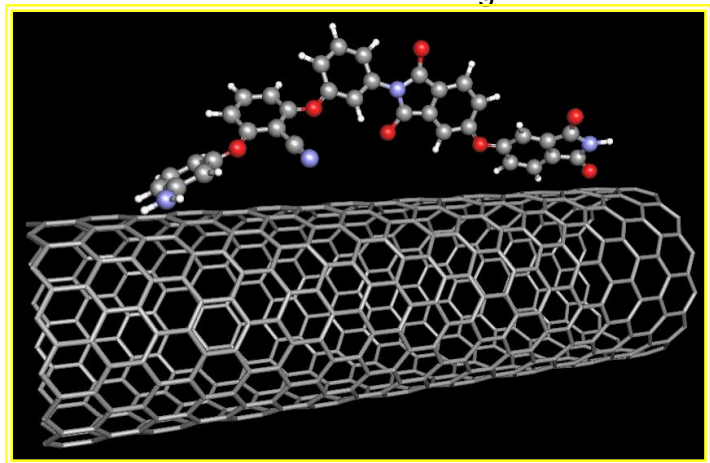
Building Blocks: SWCNT/Polymer Nanocomposites

Electroactive High Performance Polyimide

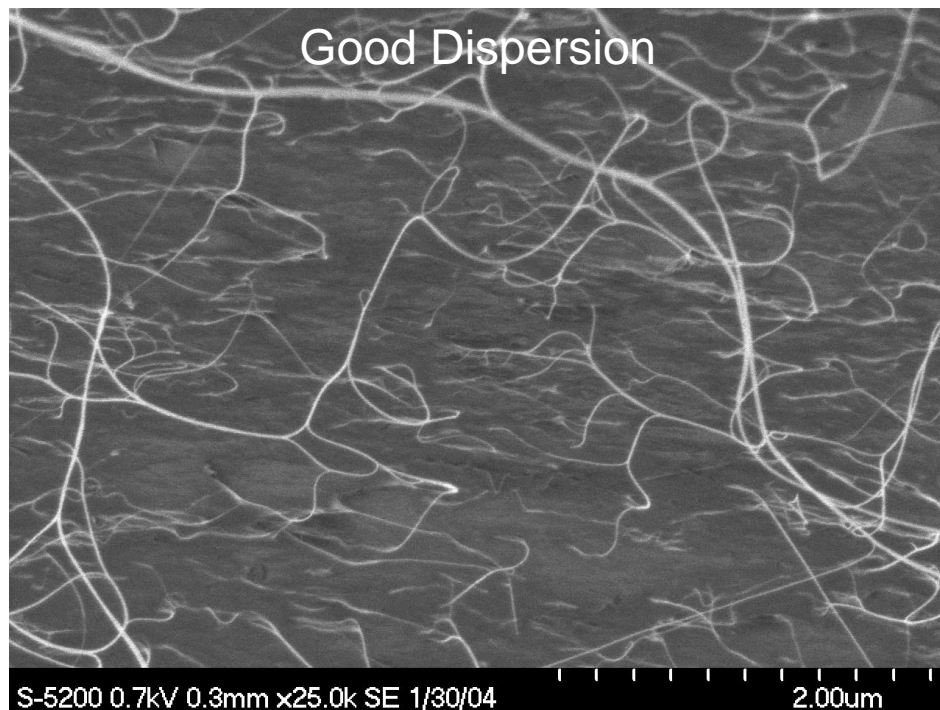
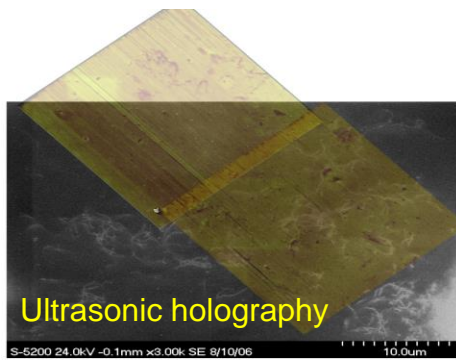
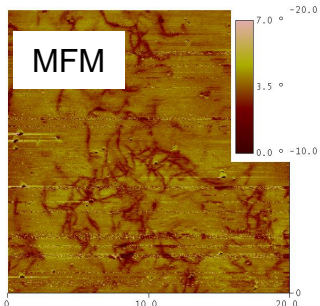


- Dispersion Interaction
- Donor-Acceptor interaction
- In-situ Polymerization under sonication and shear

(β -CN)APB/ODPA ($T_g = 220^\circ\text{C}$)



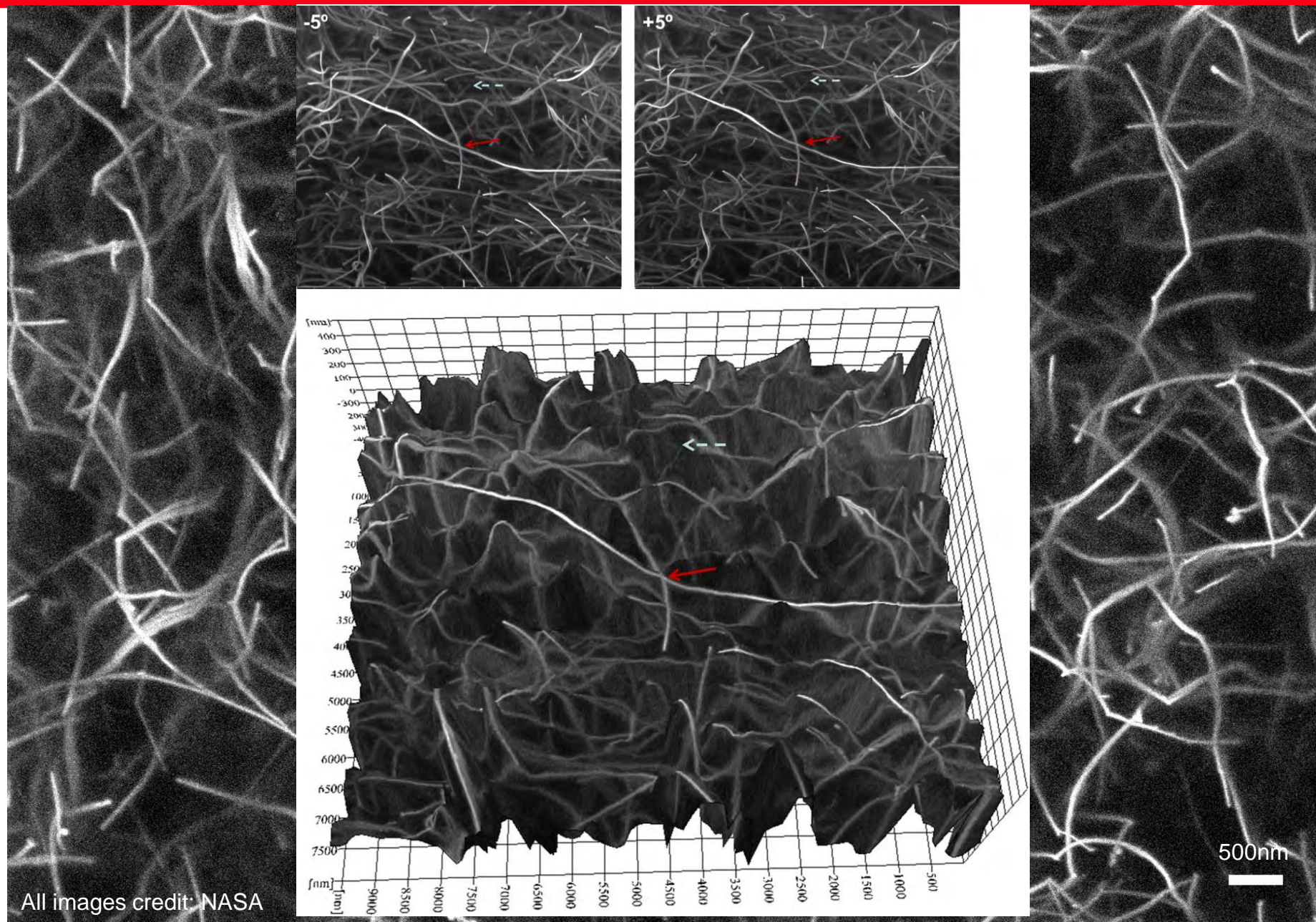
Polyimide + SWNT



Park et al, *Chem. Phys. Lett.*, 364 303 (2002)
Wise et al, *Chem. Phys. Lett.* 391 207 (2004)



HRSEM: Well Dispersed SWCNT in Polyimide (2D & 3D)



All images credit: NASA



Tailoring Physical Property for Multifunctions

Materials Properties to be Tailored

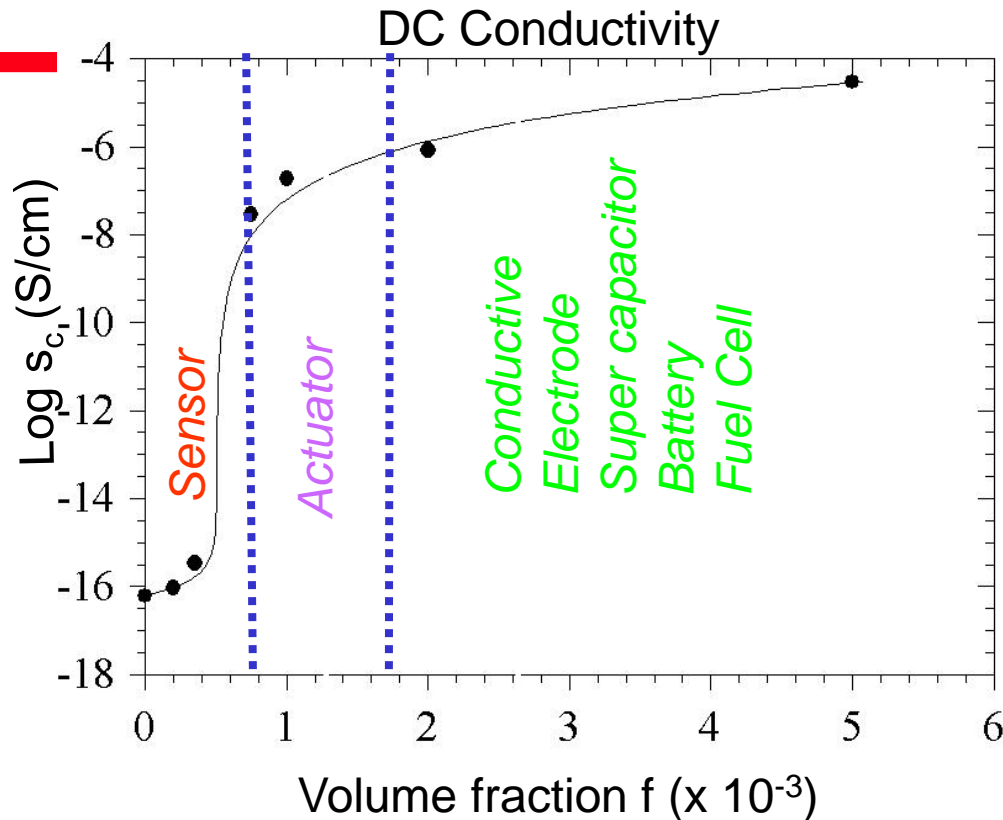
- Electrical Conductivity
- Dielectric Permittivity
- Magnetic Permeability
- Thermal Conductivity/expansion coefficient
- Radiation Shielding
- Mechanical (modulus, strength, toughness...)
- Solar Absorptivity
- Thermal Emissivity
- Band gap engineering
- Optical property (transparency, refractive index...)
- Piezoelectricity/Pyroelectricity/Electrostrictive
- Gas/Liquid Permeability
- Anisotropy/orientation

Design Parameters

- Nano Inclusion type and combination (CNT, BNNT, BCNNT, GP, hBN, NP...)
- Matrix type
- Composition
- Dispersion
- Orientation
- Geometry, Fabrication, Processing...



Versatility of SWCNT Electroactive Polymer Nanocomposites



$$(1 - f)(S_i^{1/s} - S_m^{1/s}) / (S_i^{1/s} + A S_m^{1/s}) + f(S_c^{1/t} - S_m^{1/t}) / (S_c^{1/t} + A S_m^{1/t}) = 0$$

$$A = (1 - f) / f_c$$

McLachlan et al, *J. Phys. C* 20 865 (1987), *PRB* 56 1236 (1998)

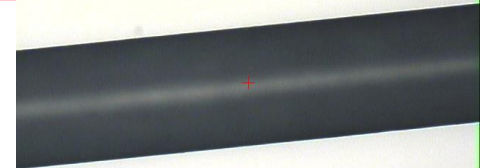
- In the vicinity of percolation, the composite acts as a dielectric material and yields an enhanced sensor response
- Above percolation, the composite is conductive (anti-static) and can be used as an electrostatic actuator
- Well above percolation, the composite is very conductive

McLachlan et al, *J. Poly. Sci.: Poly. Phys.* 43 3273(2005)

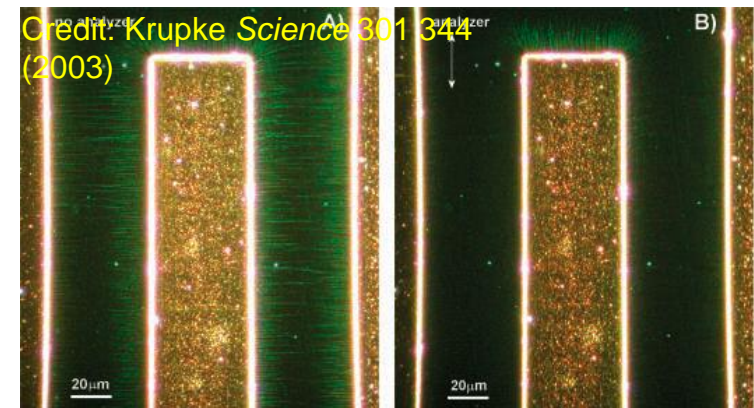
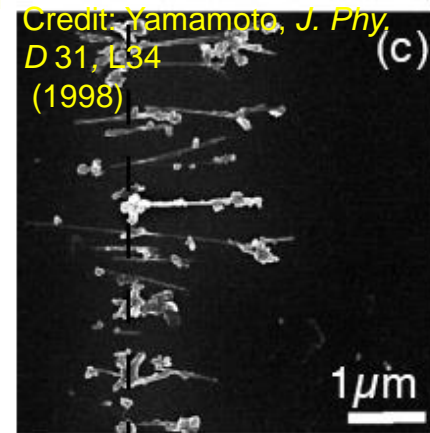


Alignment Approach

Wet spun fiber
1%SWCNT



Credit: NASA



- *SWCNT Reinforced Functional Polymer Composites*

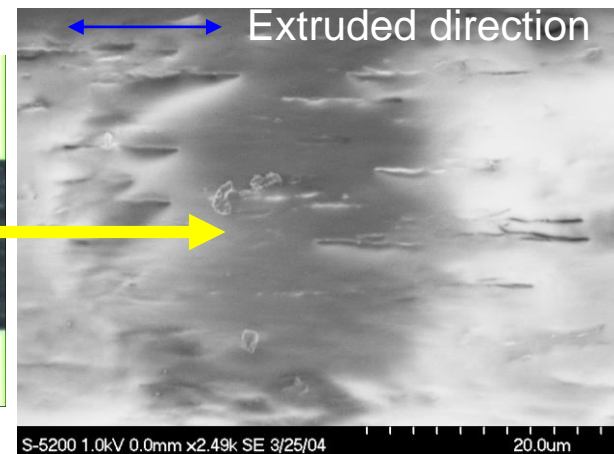
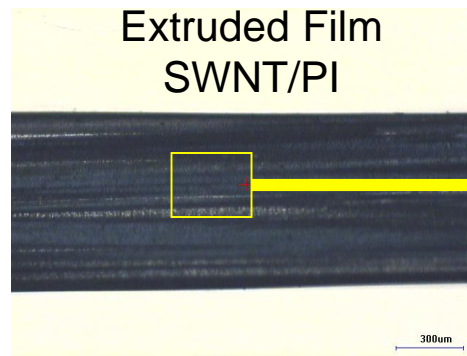
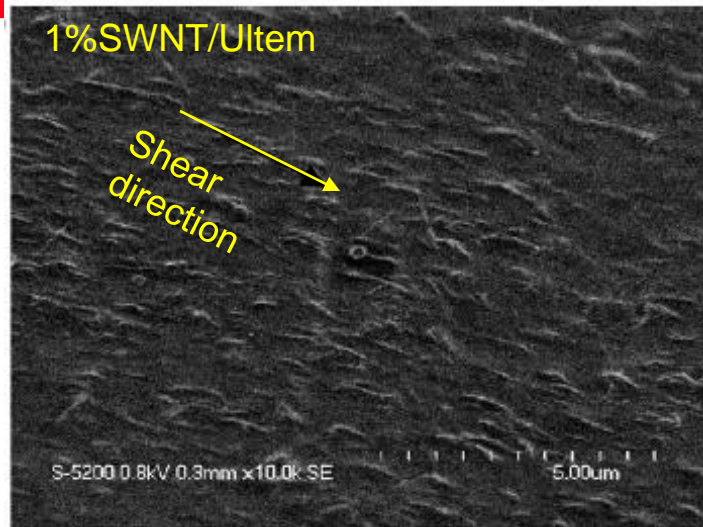
- *Alignment*

- *High Shear Alignment (Passive)*
 - Extrusion, Pultrusion, Calendering
 - Fiber spinning (melt and wet spinning)
 - Electrospinning
- *Electric Field Alignment (Active)*
 - AC & DC in a solvent
 - CNT growth w/ EF
- *Magnetic Field Alignment (Active)*
 - MF in a solvent

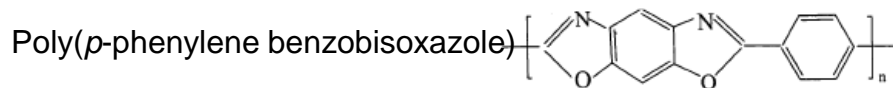
- *Aligned SWCNT-Functional Polymer Composites Using Dielectrophoresis*
Tailoring Physical Properties (Mechanical, Electrical, Dielectric, Thermal...)



Shear Alignment: Extruded Fibers and Films



Composites: *B*, 35 439 (2004)



Dry-jet wet spinning

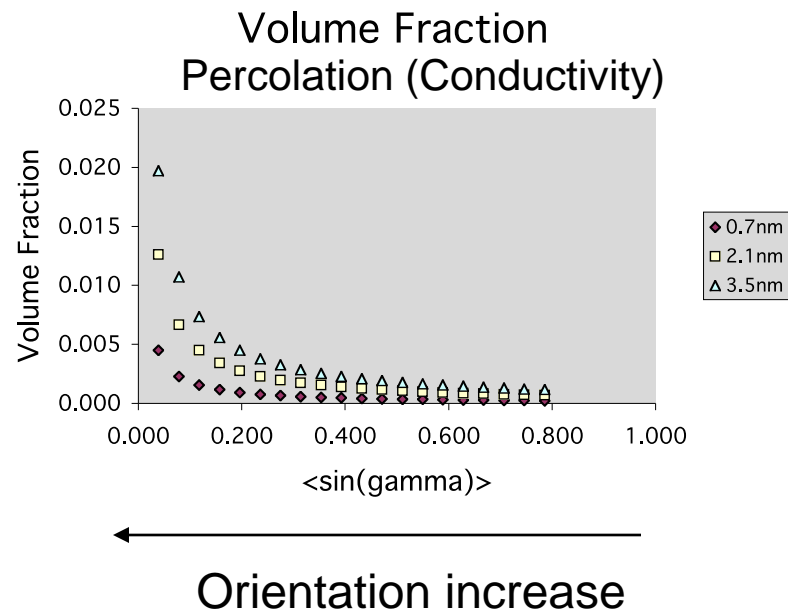
Georgia Tech Fiber	Yield strength (GPa)	Tensile mod (GPa)	Elongation (%)	Conductivity (S/cm)
PBO	2.6	138	2.0	insulating
5wt% SWCNT/PBO	3.2	156	2.3	insulating
10wt% SWCNT/PBO	4.2	167	2.8	insulating

Macromolecules 35 9039 (2002)

Percolation concentration of well dispersed SWCNT in a polyimide $\approx 0.05\text{vol}\%$

Comp. Sci. Tech. 63 (2003) 1637

Chem. Phys. Lett., 364 (2002) 303.

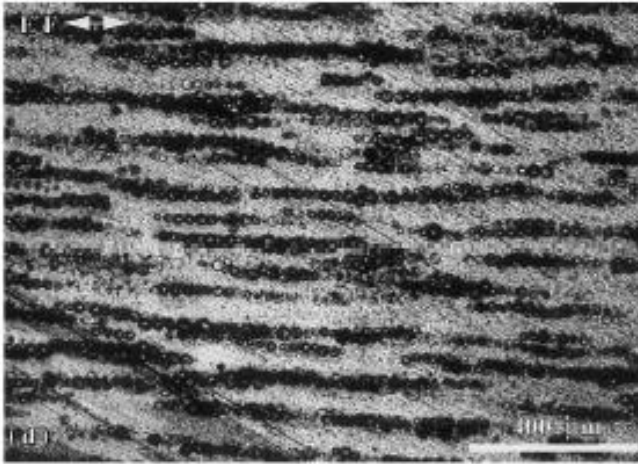


All images credit: NASA

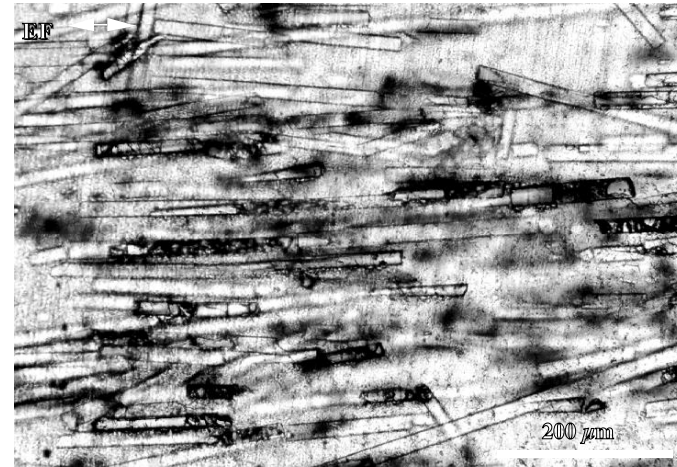


Dielectrophoretic Alignment: Spheres, Platelets, Fibers... AC Electric Field Alignment

Spheres



Fibers



Model for longitudinal and lateral aggregation of inclusions

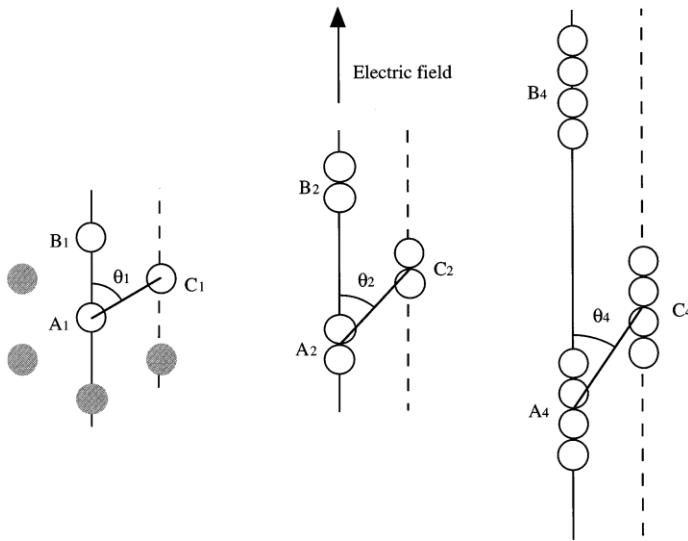


Figure 14. Optical micrograph of thin section of aligned glass fibers (4.5 vol%). Polymerized after 30 s under 0.81 kV/mm AC.

$$\beta = \frac{pe_0e_1a^3(bE)^2}{k_B T} > 1 \text{ for Alignment}$$

$$\beta = (\epsilon_2 - \epsilon_1)/(\epsilon_2 + 2\epsilon_1) \text{ or } (\sigma_2 - \sigma_1)/(\sigma_2 + 2\sigma_1)$$

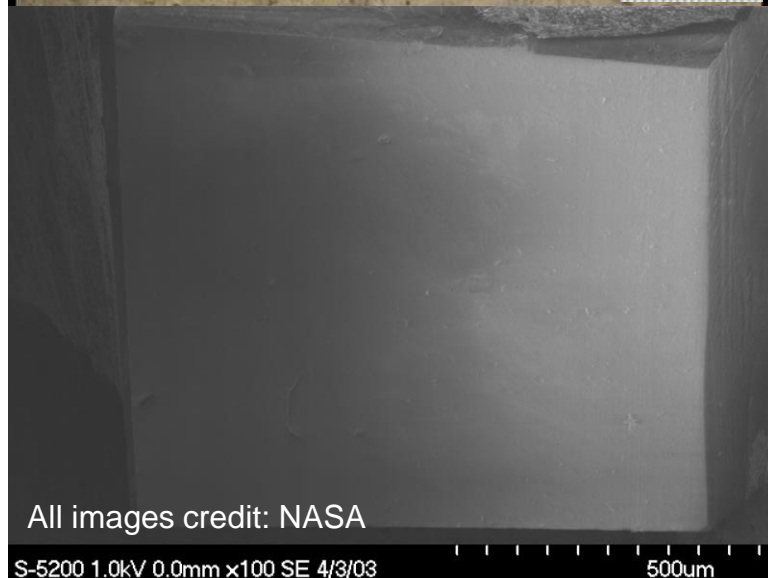
Davis, *J. Appl. Phys.* 72, 1334 (1992)

Park and Robertson, *J. Mater. Sci.*, 33, 3541 (1998)

Images Credit: Park and Robertson, *Mater. Sci. Eng.*, A257, 295 (1998)

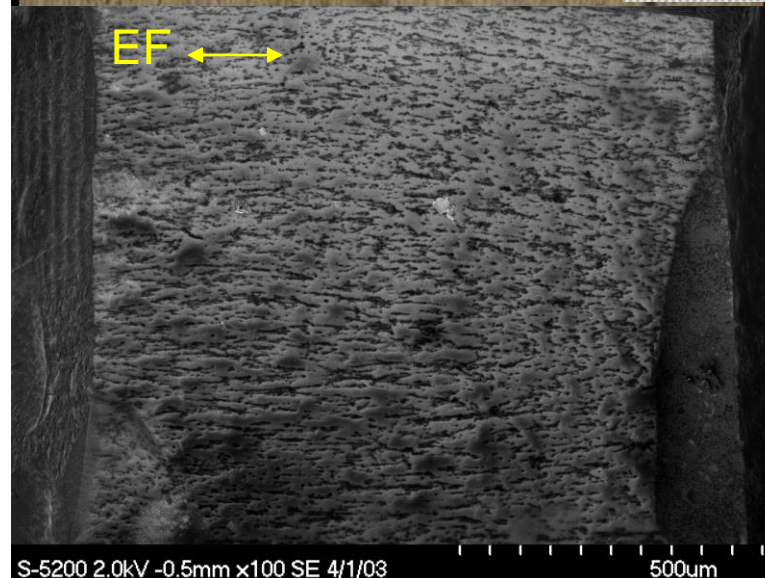
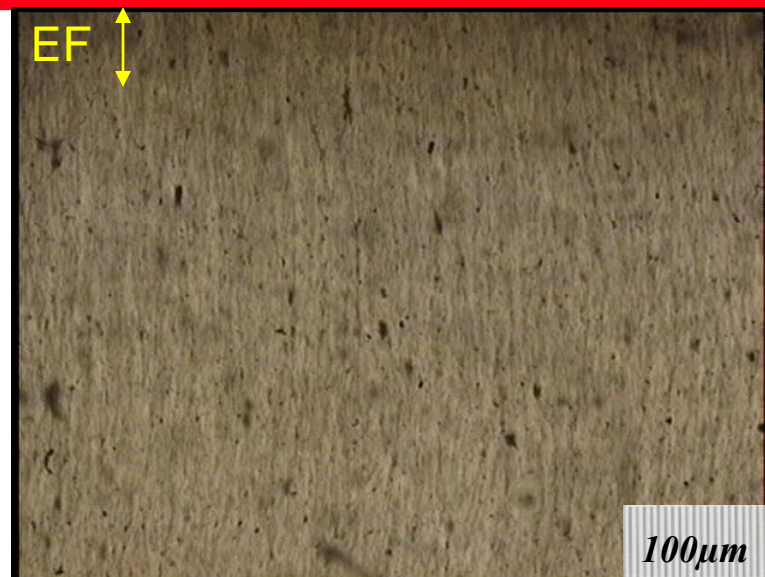


Aligned SWCNT/Polymer Composites: OM and SEM



Cured without electric field

SWCNT loading: 0.03wt%



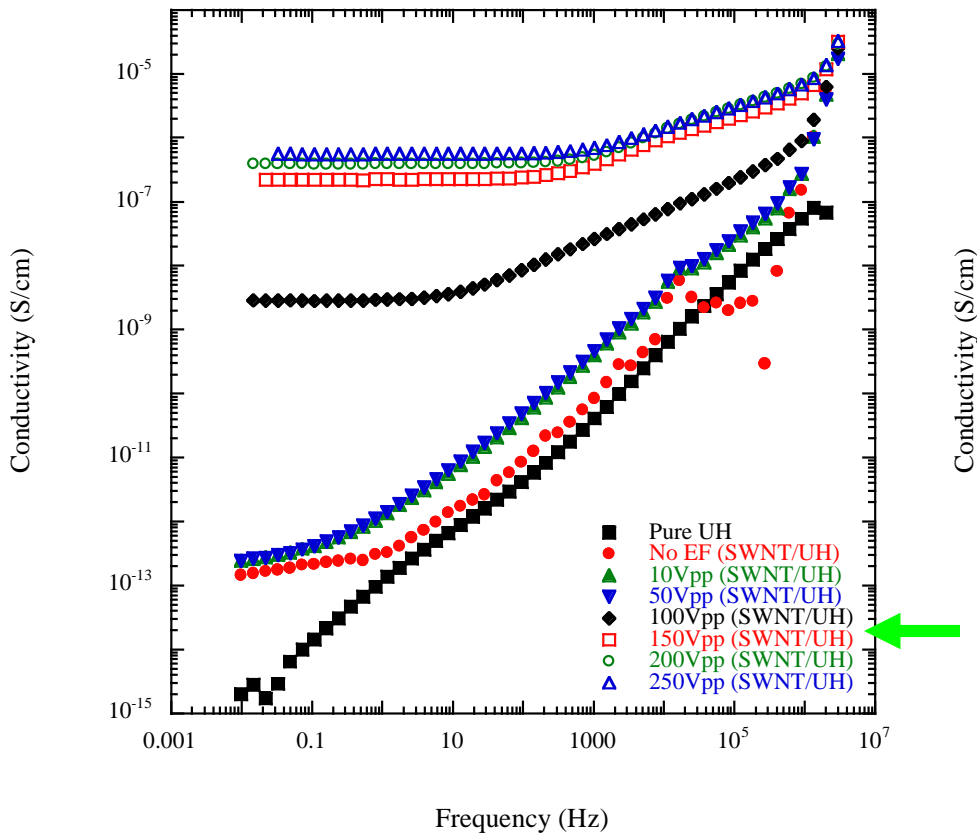
Cured with electric field (200V_{p-p}, 10Hz, 10min)

Park et al, *J. Poly. Sci: Poly. Phys.* 44 1751 (2006)

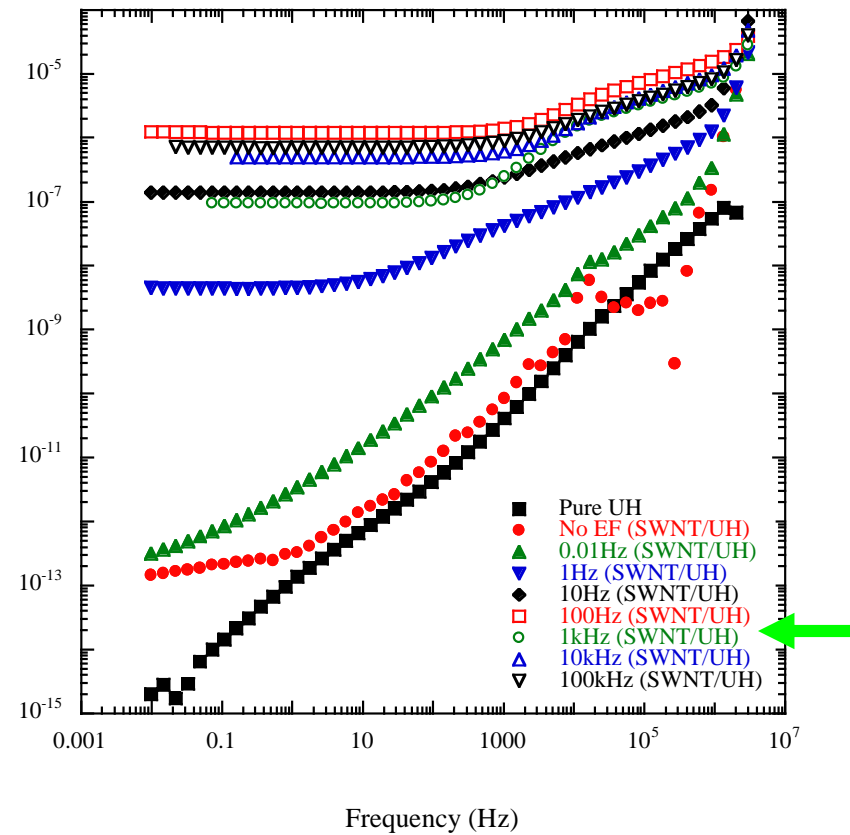
Effect of Alignment of 0.03%SWCNT/Polymer Composites

$$0.03\% < \phi_c$$

Applied Voltage



Frequency

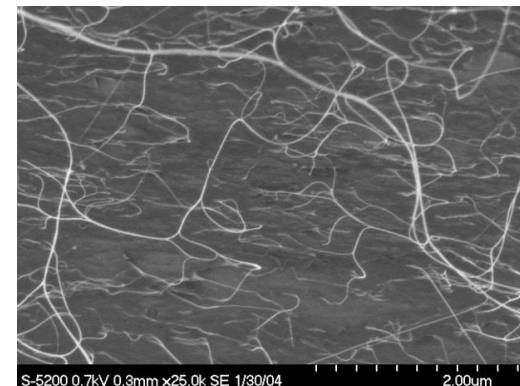
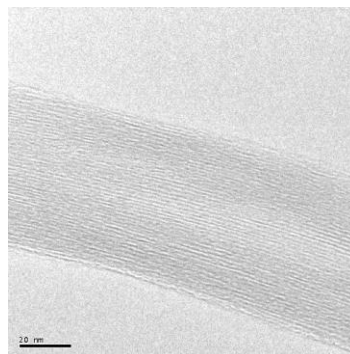
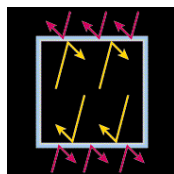
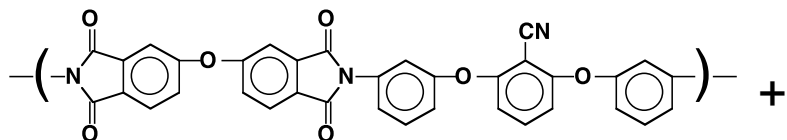


Degree of SWCNT Alignment ==>> Tailor Physical Properties

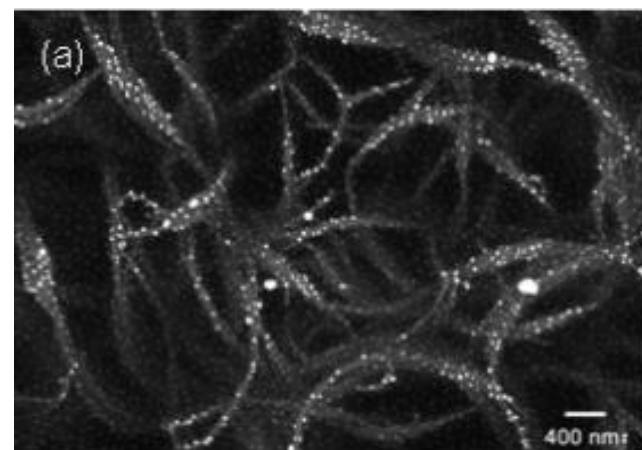
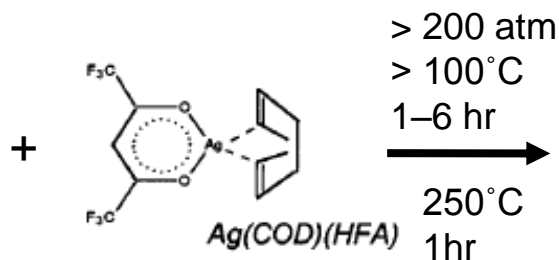
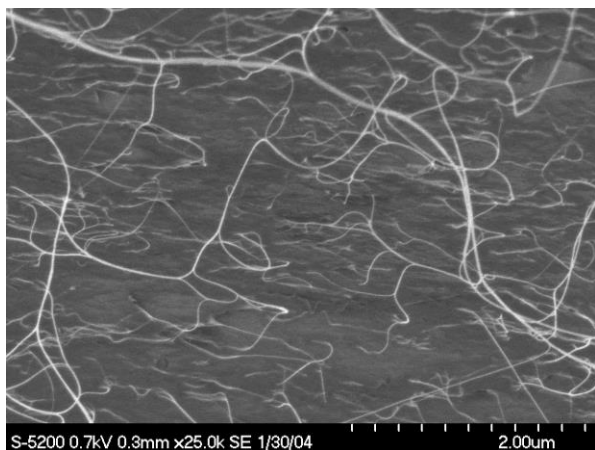


Metallized Nanotube Polymer Composite (MNPC) Metal Infusion Process into SWCNT/Polyimide Film

SWCNT/polyimide film formation: good dispersion

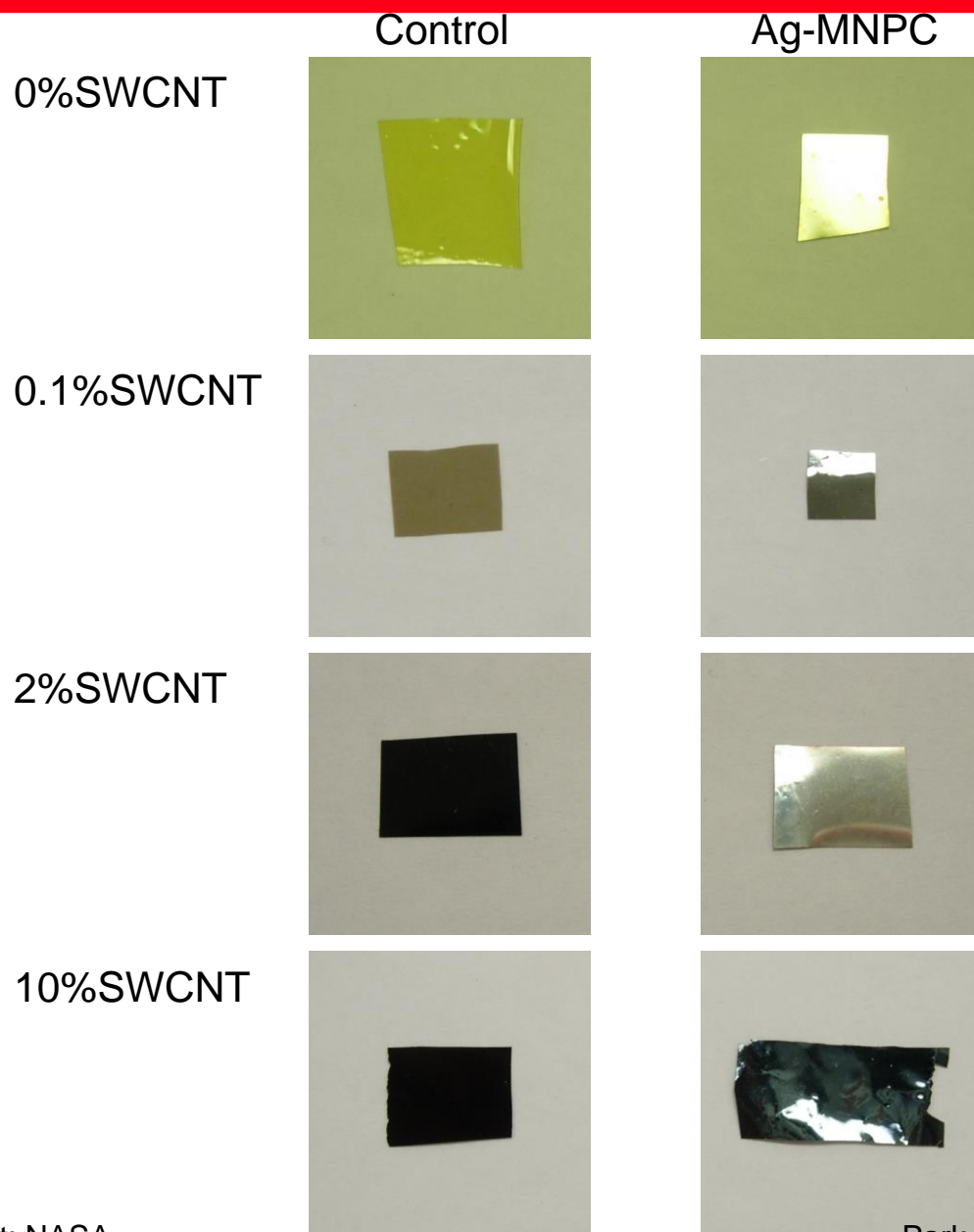


Metal-MNPC (Metal/SWCNT/polyimide) film formation: SCF Metal impregnation





Ag-MNPC Films with various SWCNT Concentration

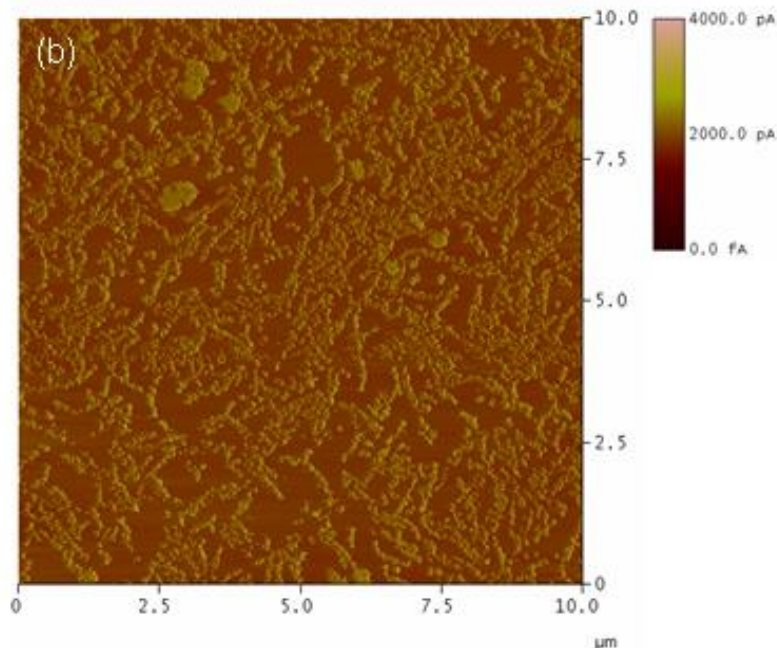
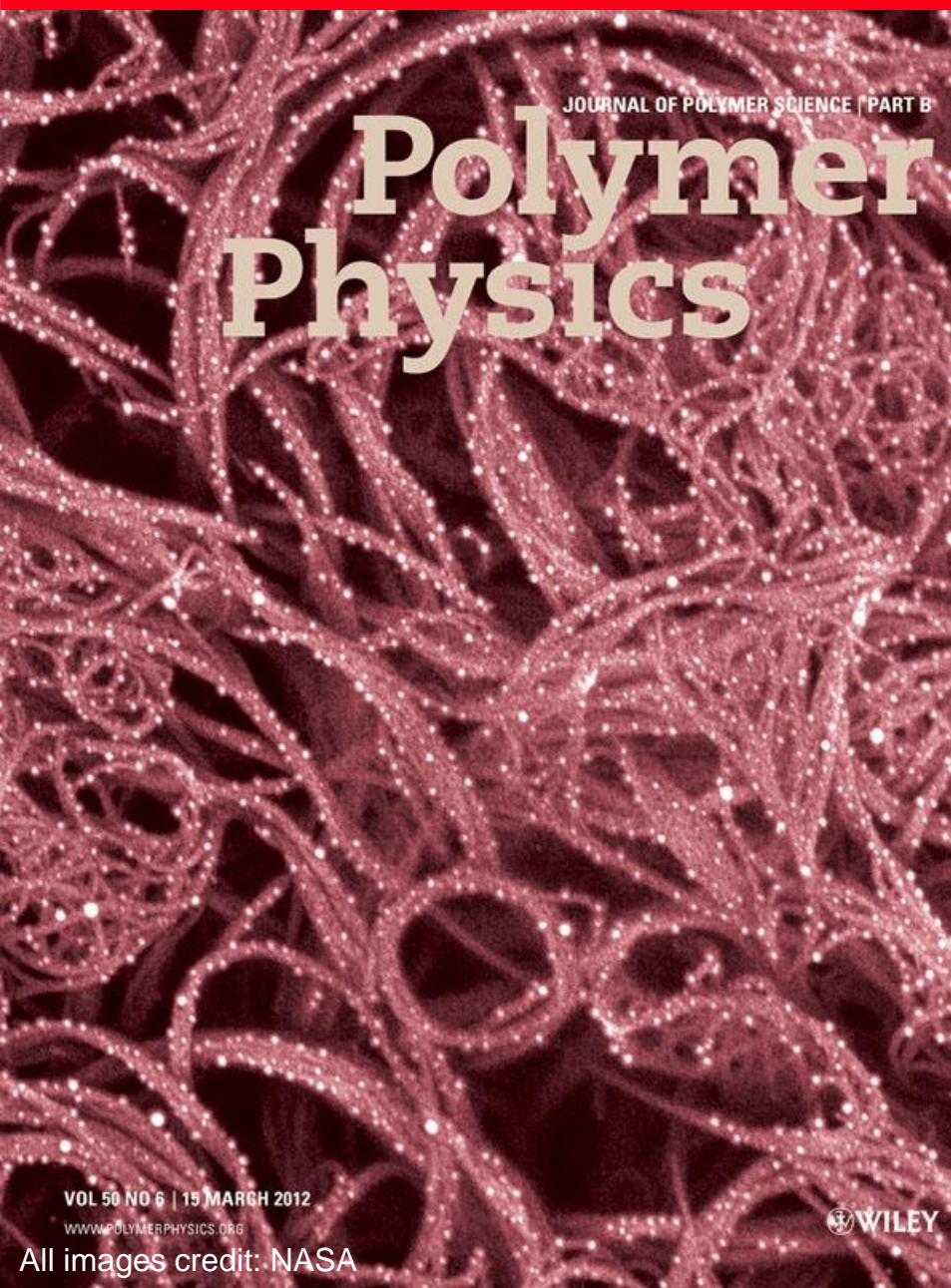


Shiny surfaces
Reflection shielding





Tunneling AFM & HRSEM: Ag-MNPC: Ag/10%SWNT/ β CN AO



Above: Topograph and tunneling AFM images of 10 wt.% SWNT/ β -CN AO/Ag prepared by 20 % metallization solution.

Conductivity & Toughness increased

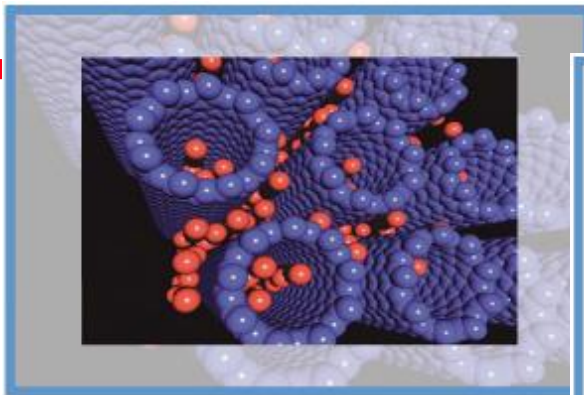
Left: HRSEM micrograph of 10 wt.% SWNT/ β -CN AO/Ag prepared by 20 % metallization solution.

Credit: *J. Poly. Sci.: Poly. Phys.*, 50, 394 (2012)

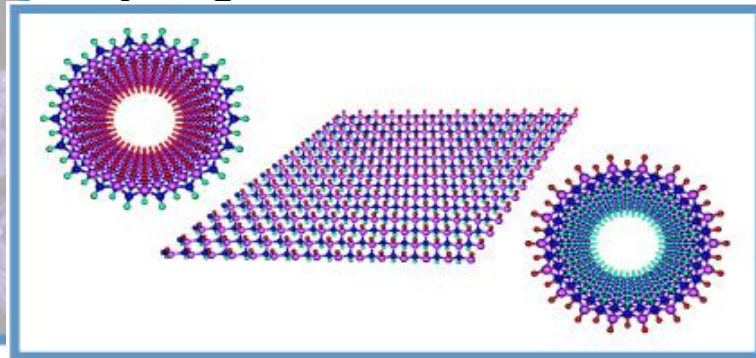


BNNT enables.....

Hydrogen Storage BNNT

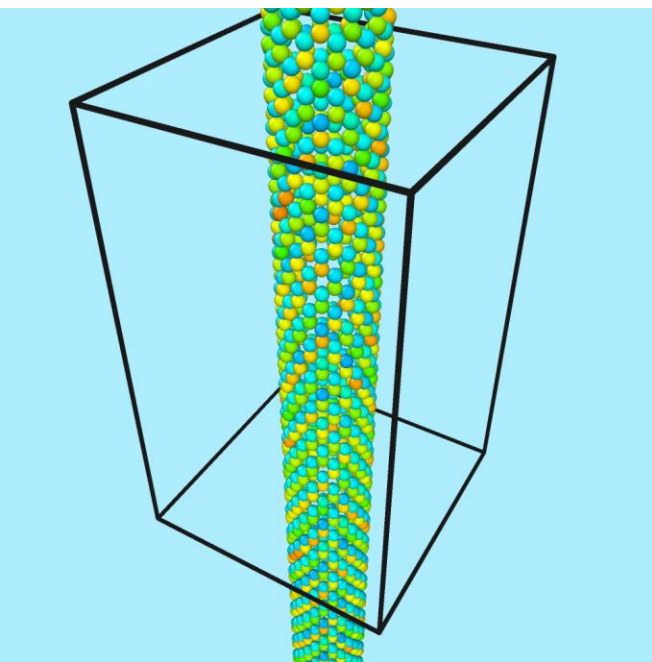


Hydrogenated BNNT

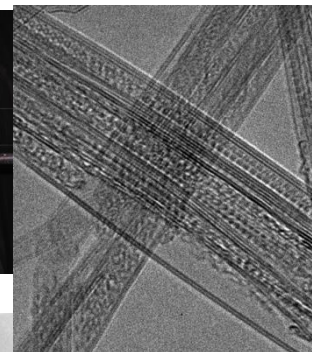
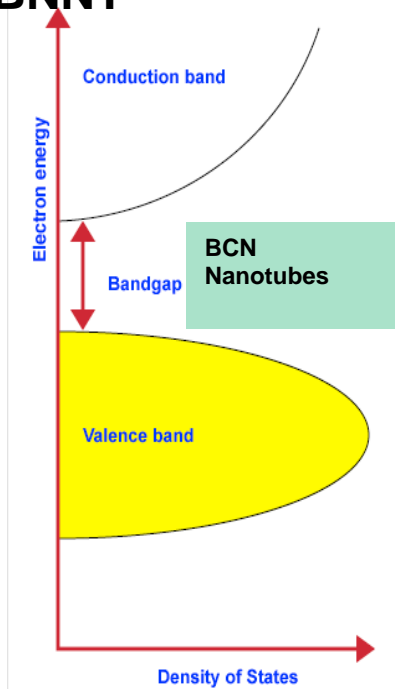


Radiation Shielding Materials Containing Hydrogen, Boron, and Nitrogen: Systematic Computational and Experimental Study

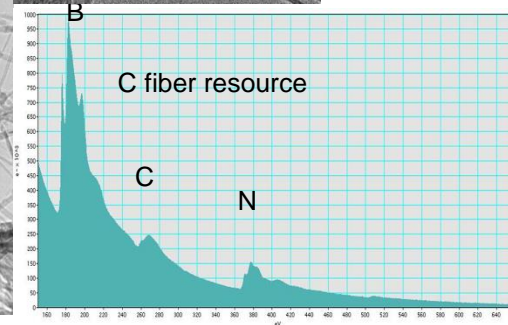
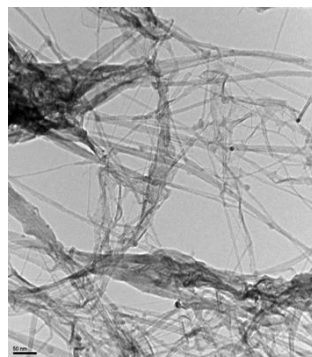
Electroactive properties of BNNT



BNNT (12 0) Polarization in Stretching
Induced Electric charge (e)



TEM image of C₆₀
BNNT
(endo-doped)
UC Berkeley



TEM, EELS, and Raman spectra of BCNNT.

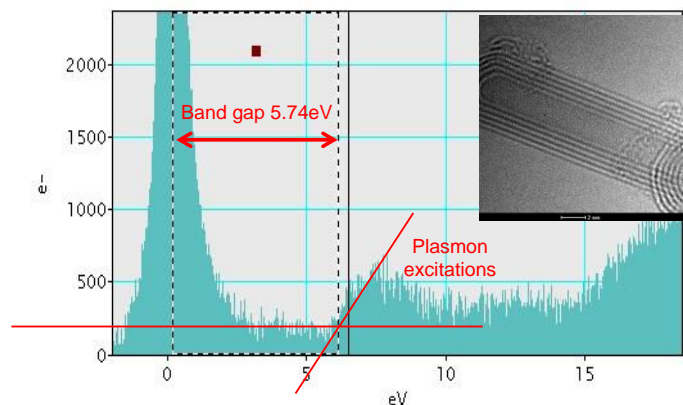
$B_xC_yN_z$ Nanotube (BCNNT) Development

All images credit: NASA

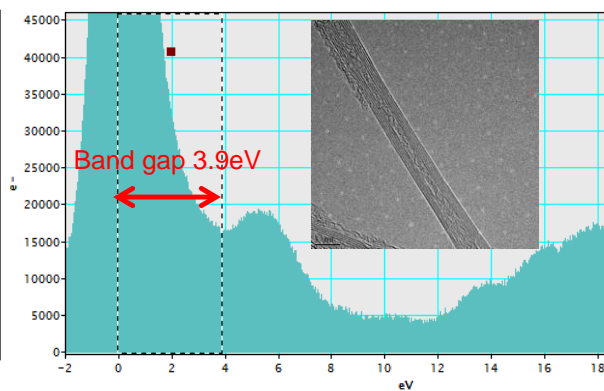
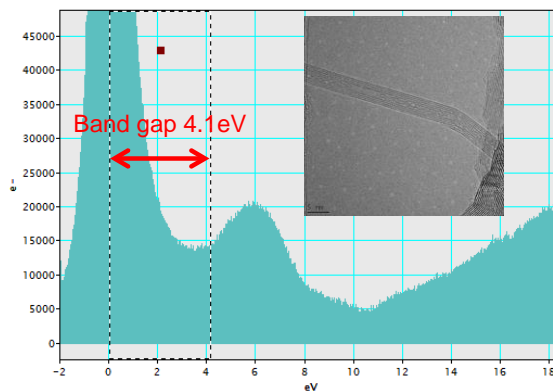


Band Gap Measurement: Low Energy EELS (modified BNNT)

Bandgap measurement of BNNT
(Low-loss region)

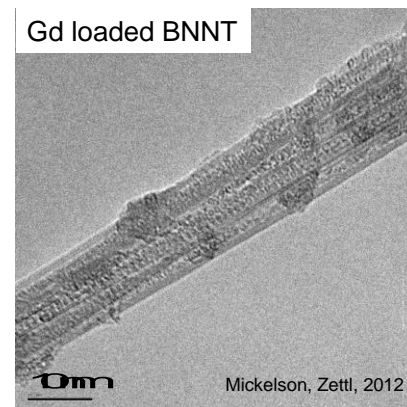
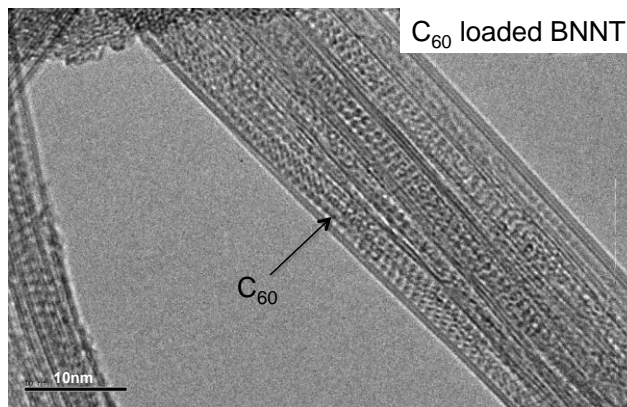
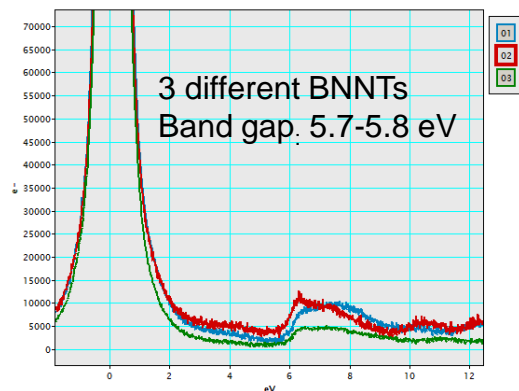


Bandgap measurement of C_{60} /BNNT
(Low-loss region)



Endo-Doped BNNNT (C_{60} /BNNT, Gd/GNNT)
UC Berkeley

Superimposed Low Loss EEL spectra of multi walled Boron nanotubes shown in previous pages



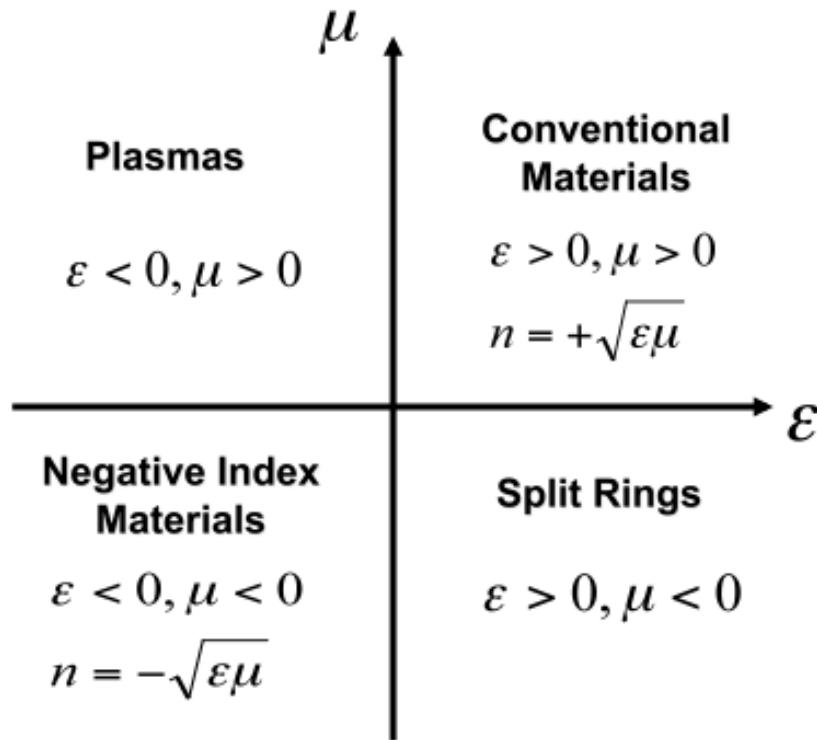
Credit: UC Berkeley; Zettl



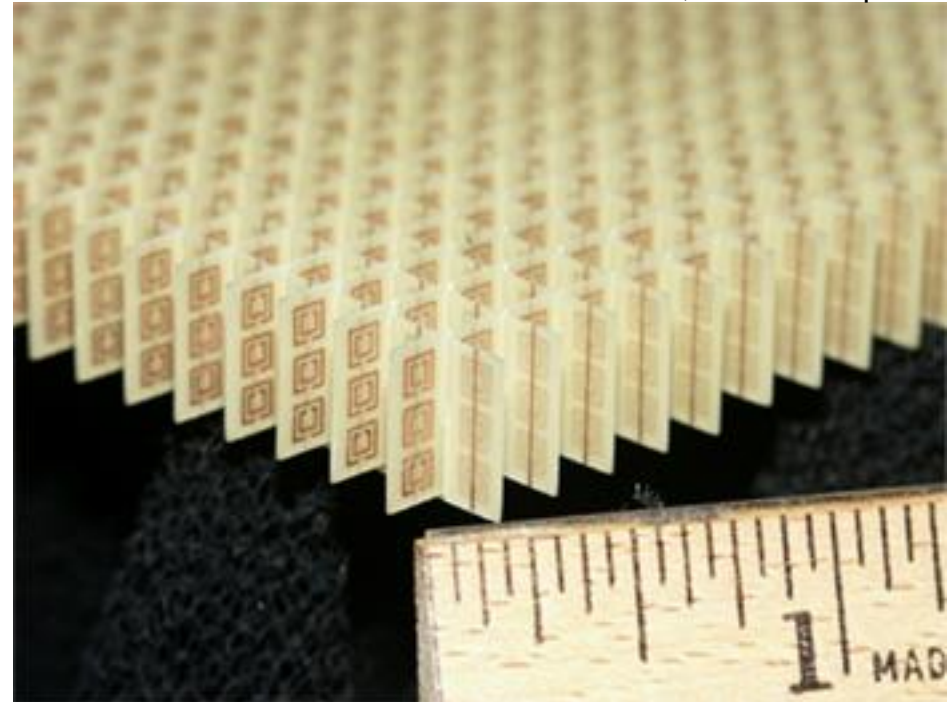
Doped Chiral Polymer Metamaterials (DCPM)



What is Metamaterial? & Challenges



$n < 1 \rightarrow$ **Metamaterials**



Metamaterials, Credit: Wikipedia

Credit: *APL* **78** 489 (2001)

Approaches

Problems of SOA Split Resonance Ring (SRR)

- Special architecture and complex design required
- Difficult to build SRR crystalline structures
- Difficult to scale-up
- Not flexible and difficult to apply for complex structures
- Difficult to reach optical ranges
- Lack of resonance frequency tunability

Metamaterials without special architecture or design (negative permeability) possible for optical ranges?

$$n_{eff} = \sqrt{em} - k$$



Novel Approach: Metamaterial without special architecture and negative permeability

Chiral Metamaterials

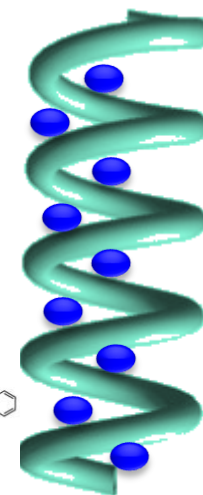
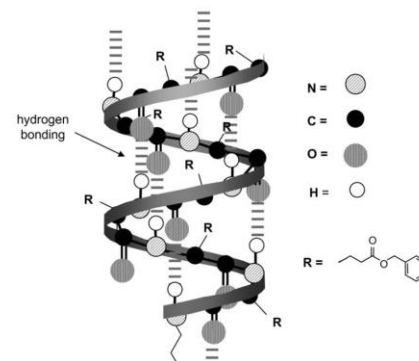
$$n_{eff} = \sqrt{\epsilon\mu} - K$$

$$K = \frac{c}{vL_v} \frac{j}{d}$$

Our Novel Approach

$$n_{eff} = n_{composite} - K_{composite}$$

$$n_{composite} = n_{host} - \Delta n_{plasmonic}$$



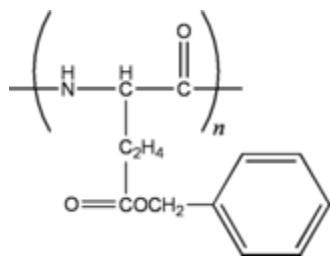
Credit: *IEEE Journal of selected topics in quantum electronics*, **10** 1154 (2004)

- The size of the **helical chiral polymer** is of the order of wavelengths in the optical range
- Self-organization of helical polymer chains
- Incorporating **plasmonic inclusions** lowers the permittivity
- Electronic coupling between plasmonic particles and helical polymer chains enhances chirality

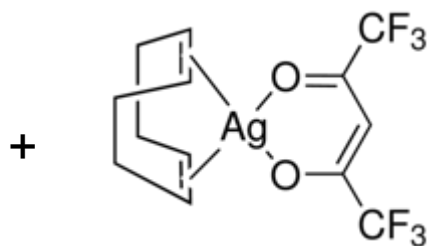
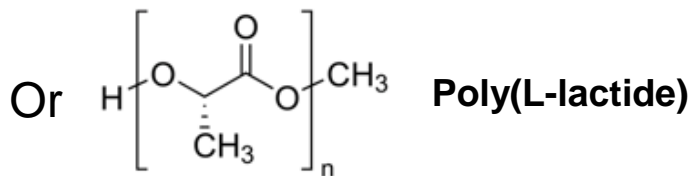


Plasmon NP infusion: *in situ* Direct Mixing & SCF infusion

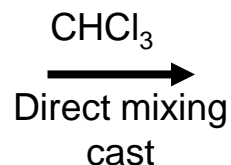
In-situ Direct mixing



PBLG



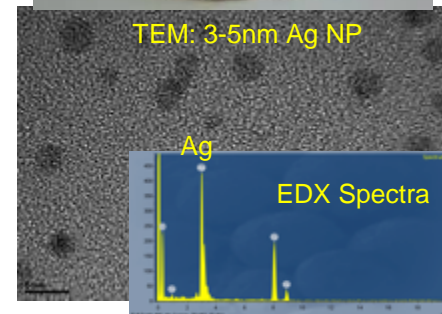
Ag salt



Ag/PBLG Film



TEM: 3-5nm Ag NP



Supercritical fluid (SCF) CO₂ Ag impregnation



PBLG Film

+

SCF CO₂



> 345.4 atm
> 70°C
1–6 hr

$\xrightarrow{200^\circ\text{C}}$
1hr
reduction



Ag/PBLG Film

All images credit: NASA

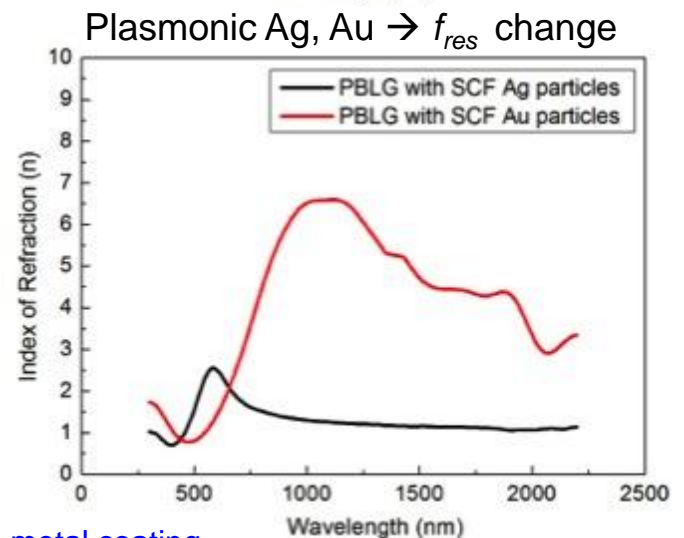
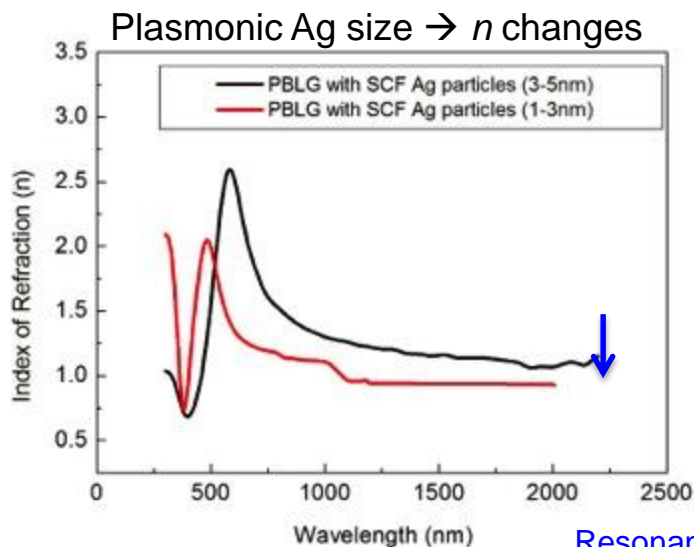
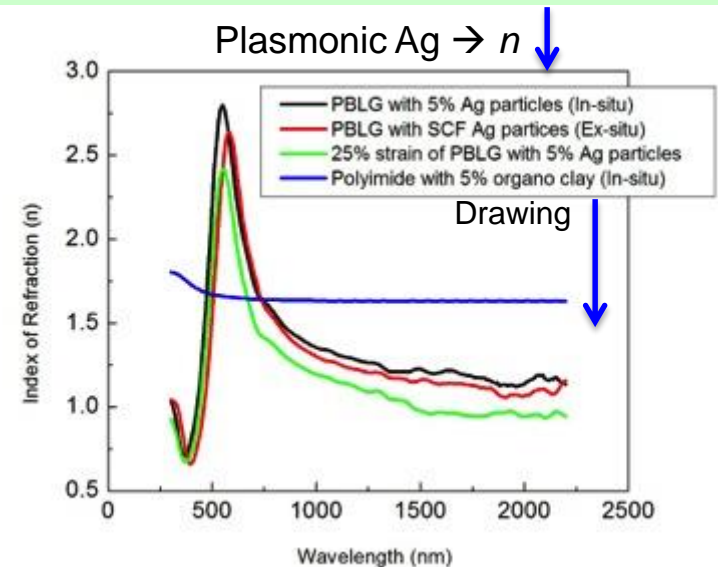
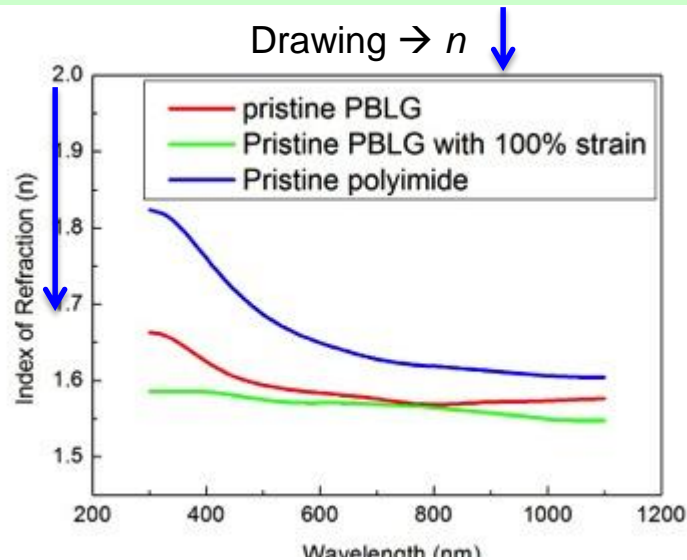


Ellipsometry (Index of Refraction): PBLG, DCPM

Drawing of chiral polymer \rightarrow Reduction of index of refraction

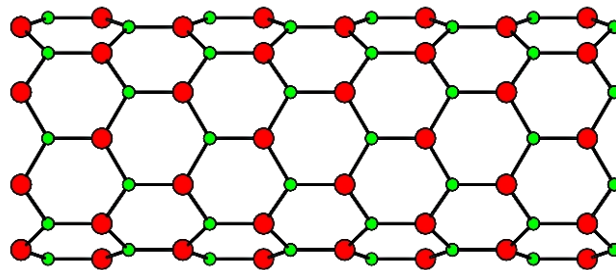
$n_{\text{PBLG}} \approx 1.55$ in visible range

Addition of Ag or Au plasmonic nanoparticles \rightarrow Reduction of index of refraction



Resonance peak is not from metal coating

Piezoelectric and Electrostrictive Properties for Sensors/Actuators (SWCNT and BNNT Composites)

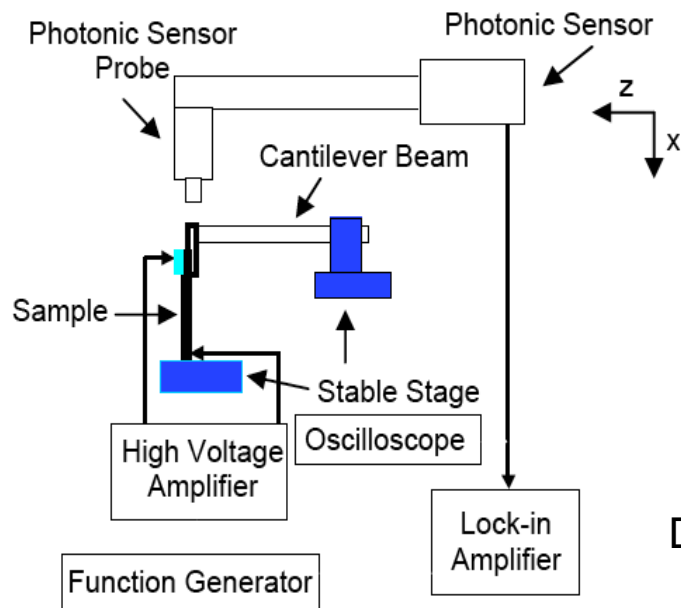
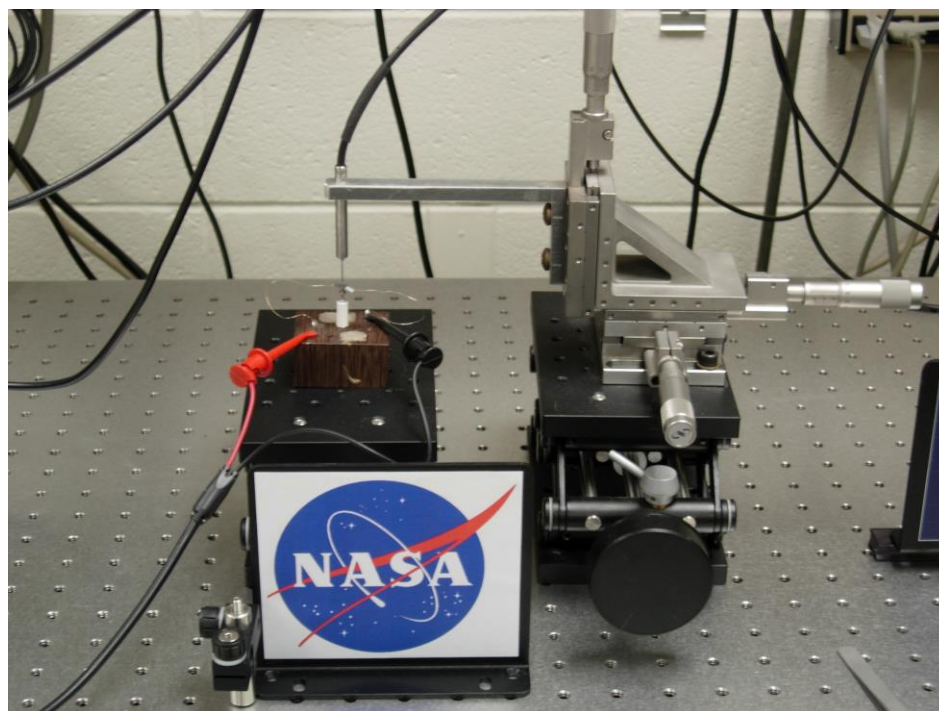
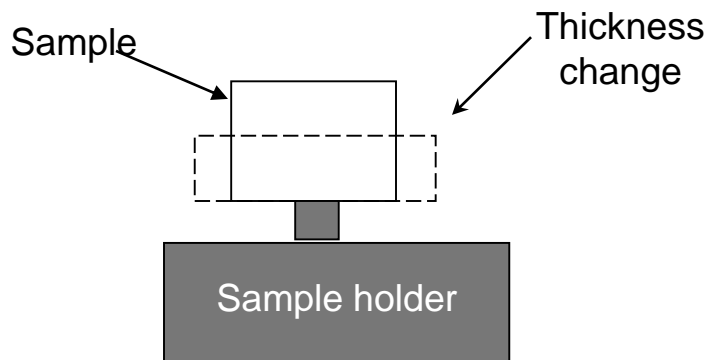




Actuation Response: SWCNT/Polyimide Composite

Out-of-plane strain

Using Fiber Optic Displacement Measurement

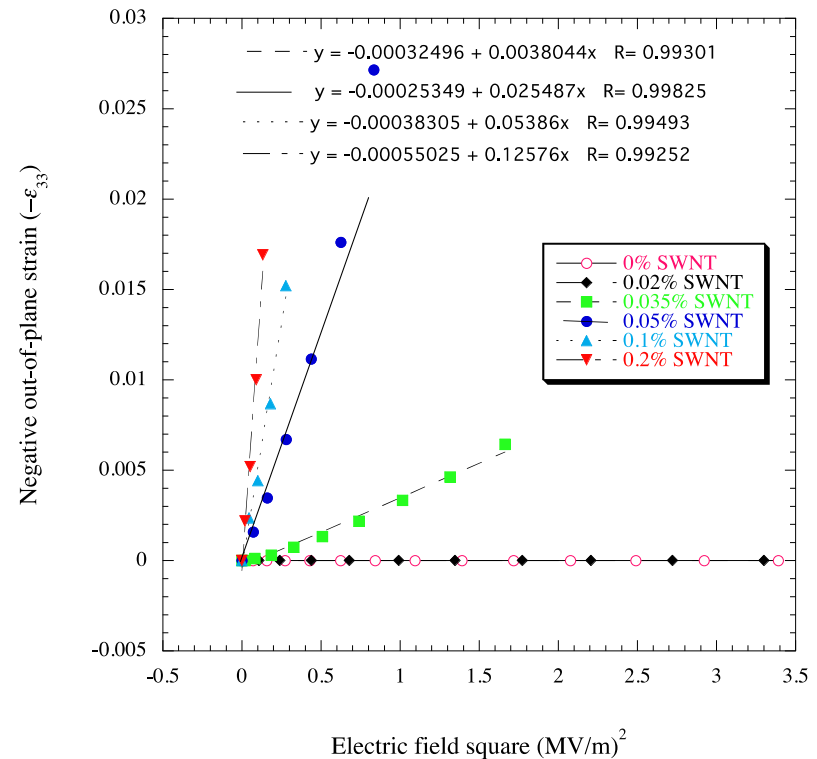
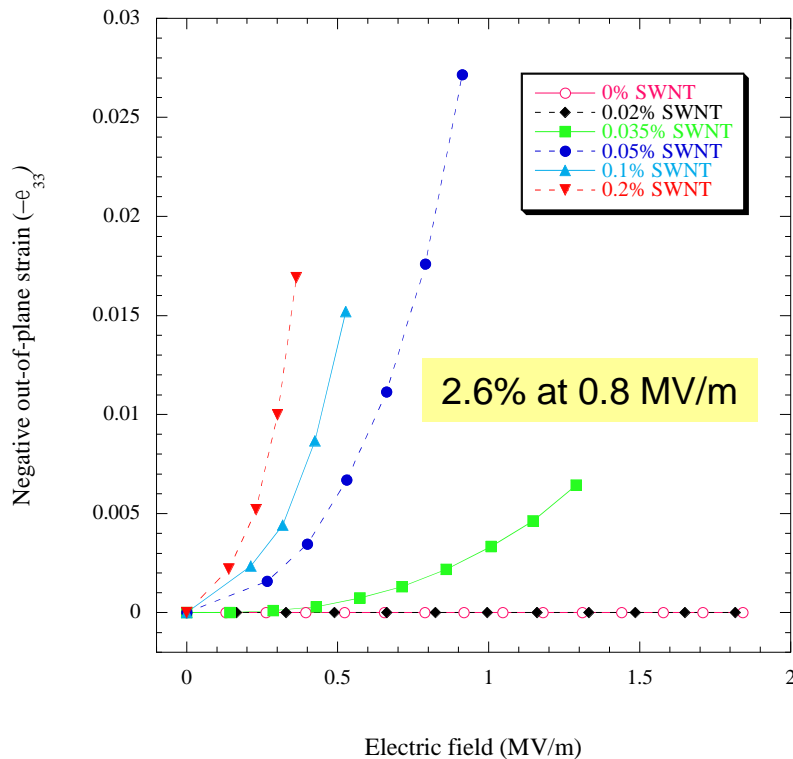


Acousto-Optic Sensors model 201
Angstrom Resolver™

Dilatometer with cantilever



Actuation: Out-of Plane Strain: SWCNT Polymer Composite



$10^3 - 10^4$ times higher

Electrostrictive coefficient

SWCNT/Polyimide $M_{33} = -3.6 \times 10^{-15} \sim -1.2 \times 10^{-13} \text{ m}^2/\text{V}^2$

Polyurethane $M_{33} = -4.6 \times 10^{-18} \sim -1.6 \times 10^{-17} \text{ m}^2/\text{V}^2$

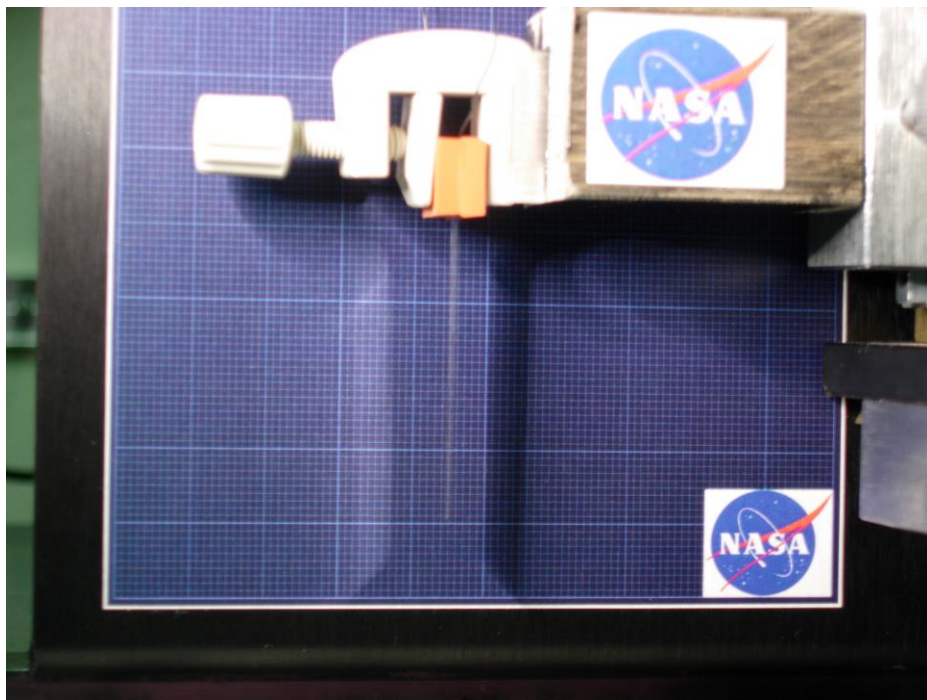
$$S_{33} = S_E (\text{Electrostriction}) + S_M (\text{Maxwell effect})$$

$$S_M = -\frac{1}{2Y} e_0 e_r E^2 (1 + 2n) < 0.01\%$$

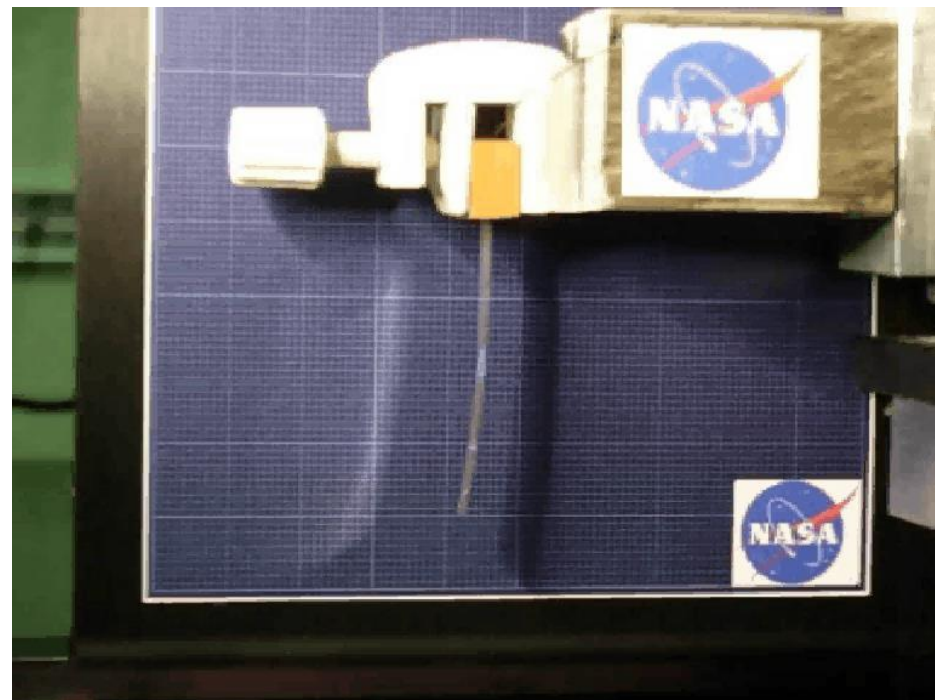


Bending Actuation of SWNT Polymer Nanocomposite

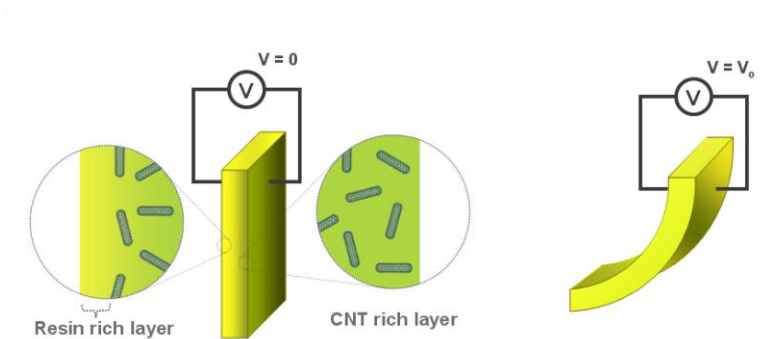
No EF



EF = 0.8 MV/m



$$M_{31} = 2.86 \times 10^{-15} \text{ (m}^2/\text{V}^2\text{)}$$



Sonic fatigue abatement
Noise transmission attenuation
Wing and panel flutter control
Tail buffet alleviation control
Surface shape control

All images credit: NASA

Park et al, *Adv Mater*, 20 2074 (2008)



Multifunctional BNNT Polymer Composites

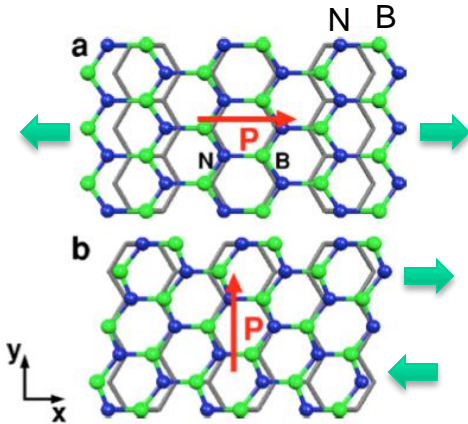
- Electroactive Properties
- Radiation Shielding Properties



Piezoelectric Properties of BNNTs

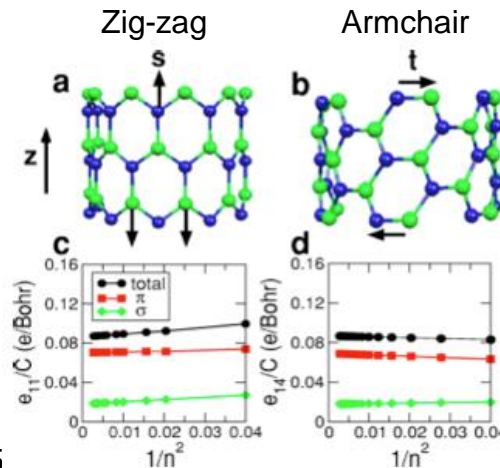
Piezoelectric Effect

h-BN plane



(Sai & Mele, PRB 68, (2003) 241405)

BNNT



Induced polarization, \vec{p} , under strain e_{jk} : $p_i = e_{ijk} e_{jk}$

where e_{ijk} - piezoelectric tensor with symmetry:

$$e_{xxx} = -e_{xyy} = -e_{yxy} = -e_{yyx}; \quad e_{xxx} = 0.086 - 0.12 e / \text{Bohr}$$

The MD model has to reproduce this behavior!

Molecular Dynamics

- Define forces between atoms using a given interatomic potential (energy)

$$U_r = \sum_{i,j} \left[\frac{1}{2} k_{ij} (r_{ij} - r_0)^2 + B_{ij} V_A(r_{ij}) \right]; \quad \vec{F}_i = -\nabla U_r / \nabla \vec{r}_i$$

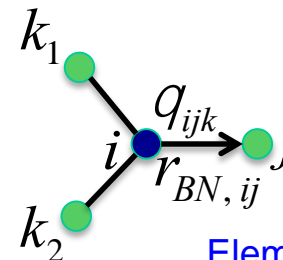
- Evolve atoms according to Newton's law: $\vec{a}_i = \vec{F}_i / m_i$

Piezoelectric MD

- Introduce dipole term to the interatomic potential (energy)

$$U = U_r + U_p; \quad U_p = \sum_{i=\{B\}, j=\{N\}} U(\vec{p}_{BN,ij})$$

$$\vec{p}_{BN,ij} = p_0 \frac{\partial}{\partial \vec{r}} \frac{r_{BN,ij} - r_0}{r_0} + \sum_{k \neq i,j} \frac{1}{2} \cos q_{ijk} \frac{\partial}{\partial \vec{r}_{ij}}$$

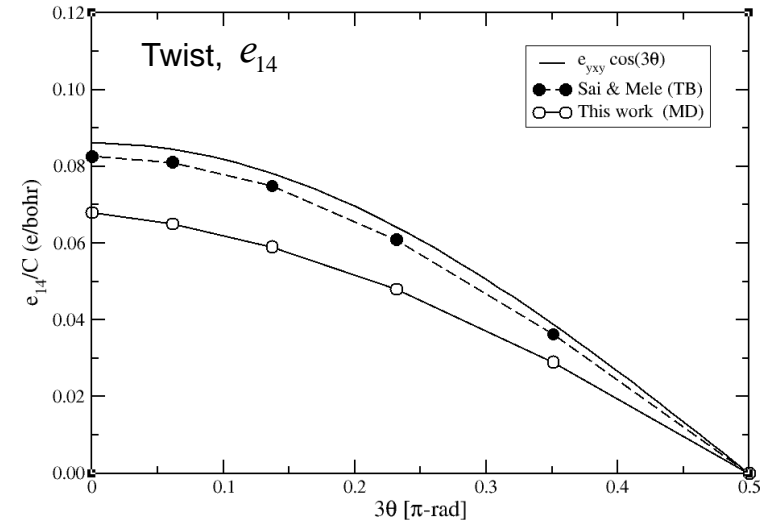
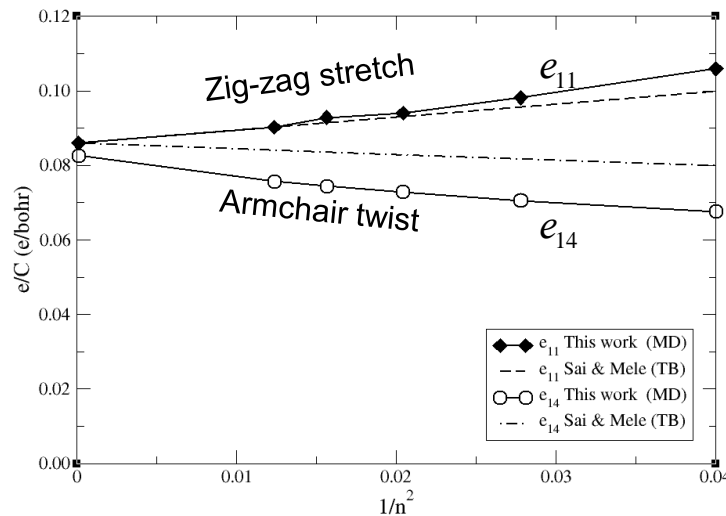
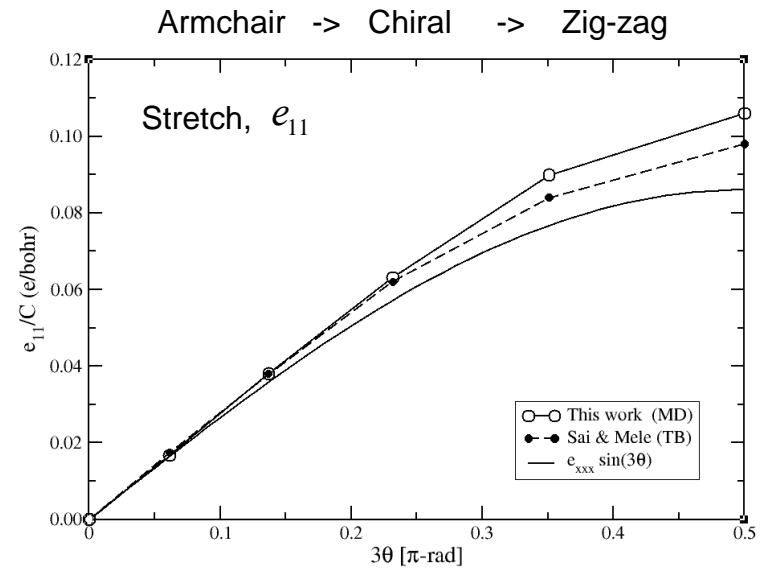
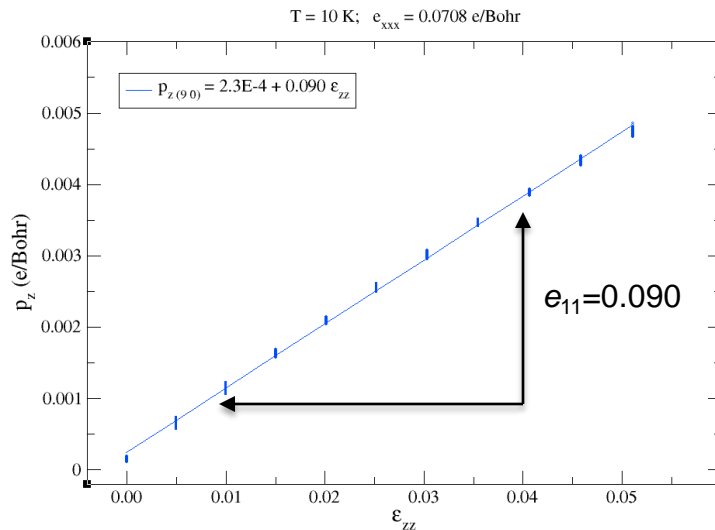
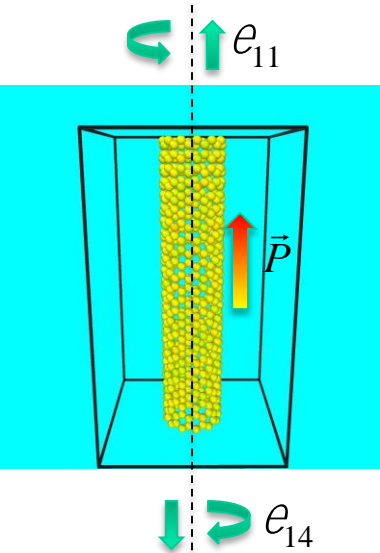


Elementary dipole unit



Results: Piezoelectricity under Deformation

The MD model is successful in representing the piezoelectric properties of BNNTs





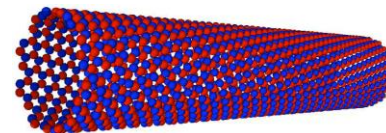
Experiment Displacement Study

Polymer Matrix:

- Polyimides [CP2, (β -CN)AMPB/ODPA (bCNAO), (β -CN)APB/PMDA (bCNAP)]
- Polyurethane
- PMMA
- Nylon 6,10

Inclusions:

- h-BN (hexagonal boron nitride powders)
- BNNT (purchased CVD, large, fat tubes, low quality)
- BNNT (high pressure, high temp, CO2 laser as grown)



Alignment (stretched)

No alignment (no stretched) and stretched (up to 100%)

Polyimide (CP2)

Polyimide (bCNAO)

Polyimide (bCNAM) (unstretched and stretched 100%)

5wt%hBN/polyimide (stretched 110%)

5wt%BNNT(CVD)/polyimide

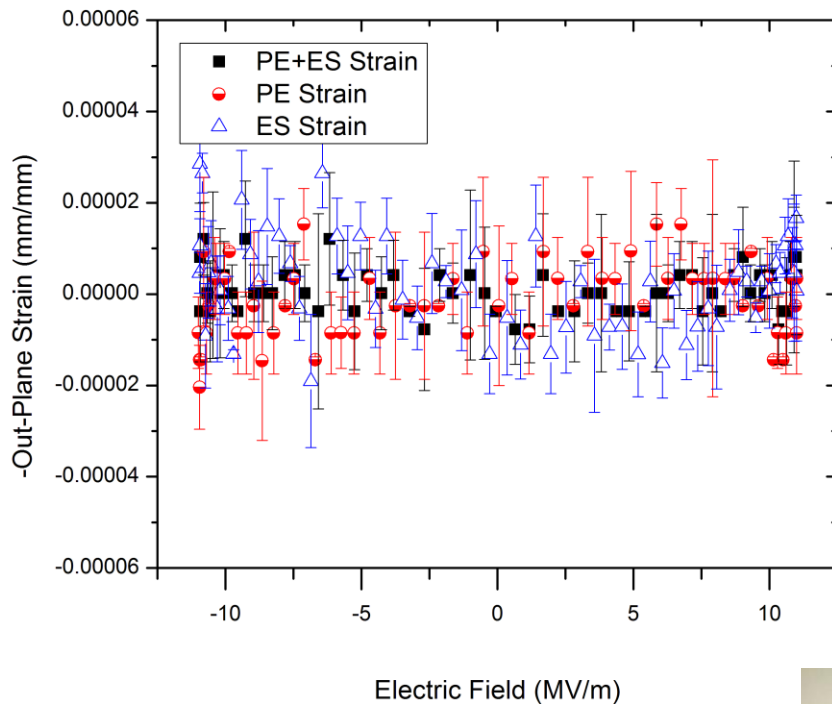
2wt%BNNT(laser)/polyimide (unstretched and stretched 100%)



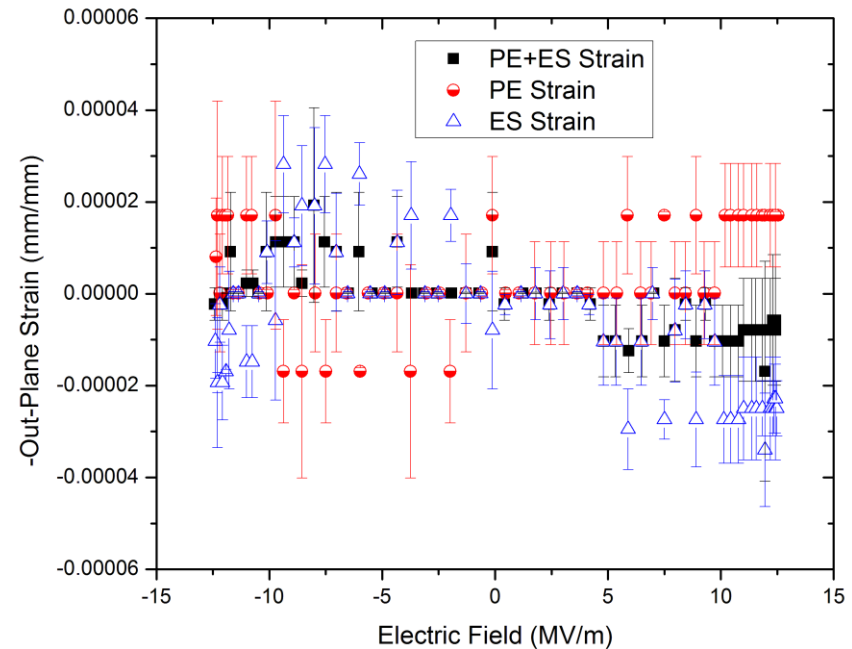
Study of Origin of Actuation: Stretched Films

Actuation of Unstretched/Stretched Pristine Polyimide

Unstretched



100% Stretched
@225°C, Annealing



Field induced strain (ϵ_{33})

$$\epsilon_{33} = d_{33} \cdot \mathbf{E} + M_{33} \cdot \mathbf{E}^2 + \dots$$

d_{33} : piezoelectric (PE)

M_{33} : mostly electrostrictive (ES)

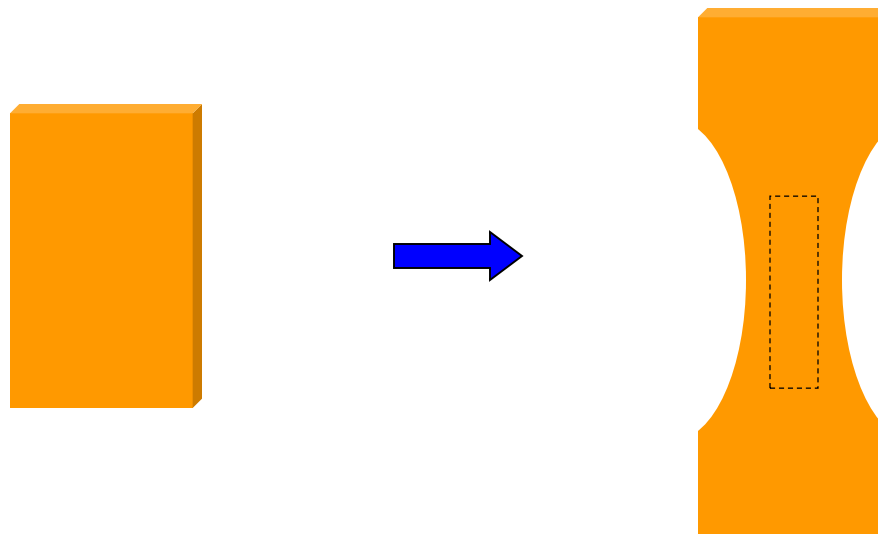


Pristine and composite films are stretched with a tensile tester (Instron microtest) in an oven at above T_g

All images credit: NASA



Stretched BNNT-Polyimide Nanocomposite

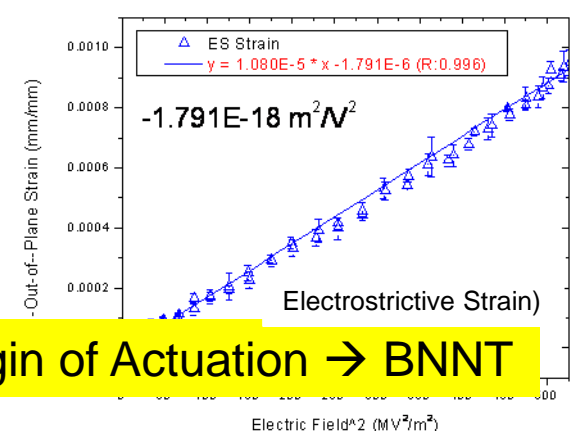
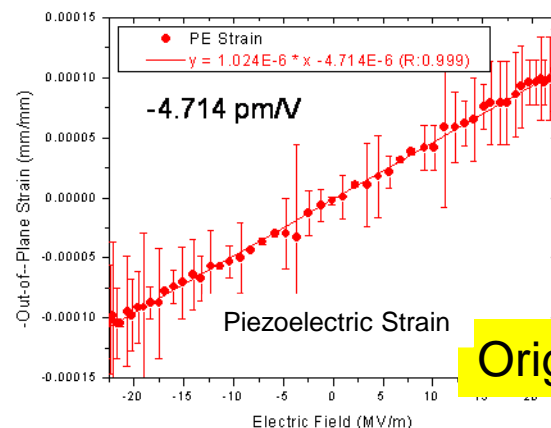
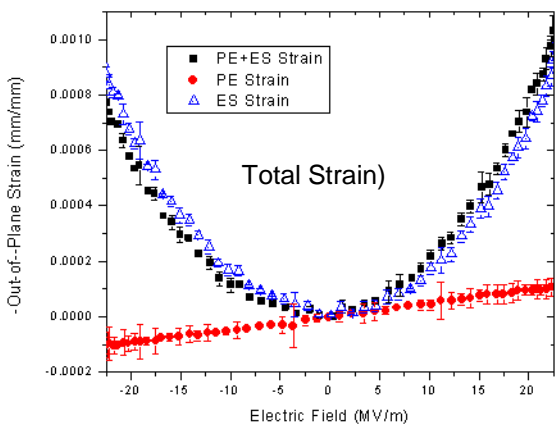
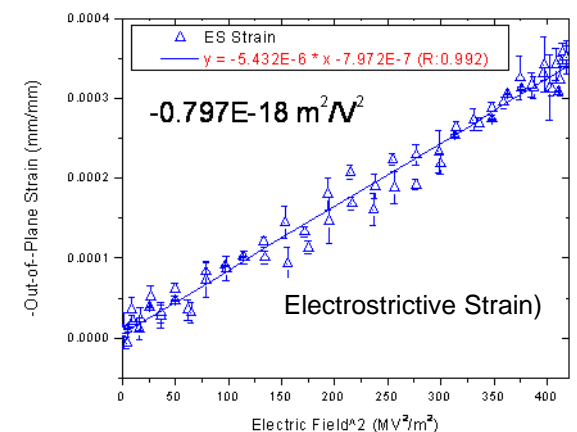
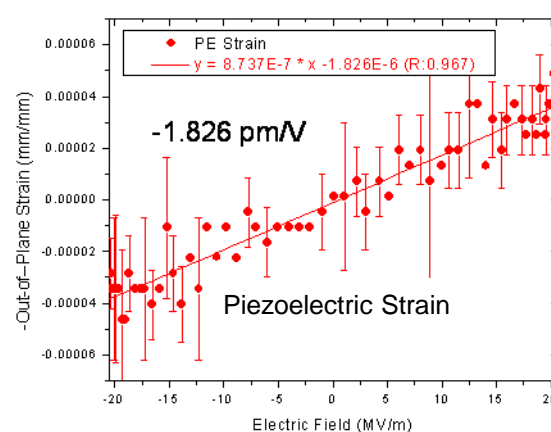
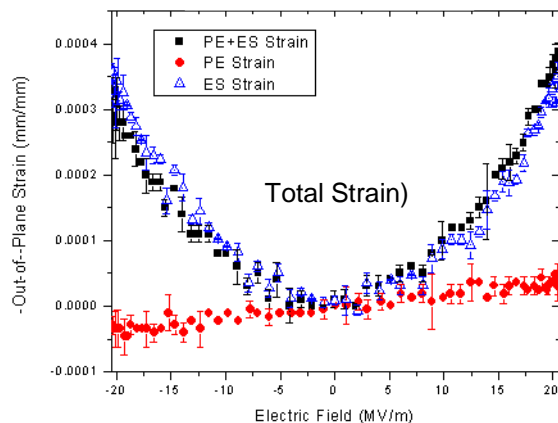
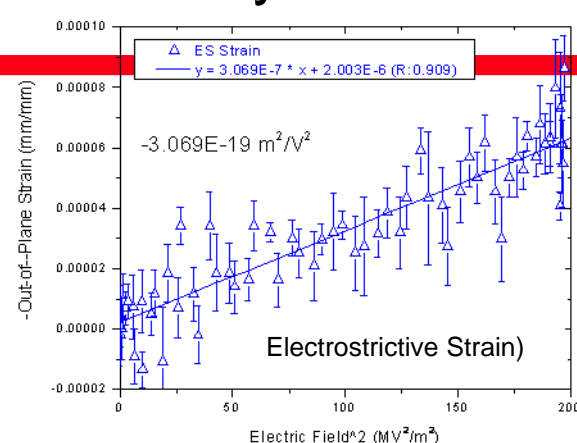
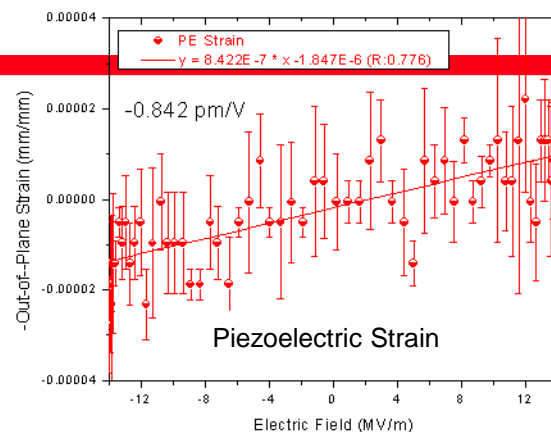
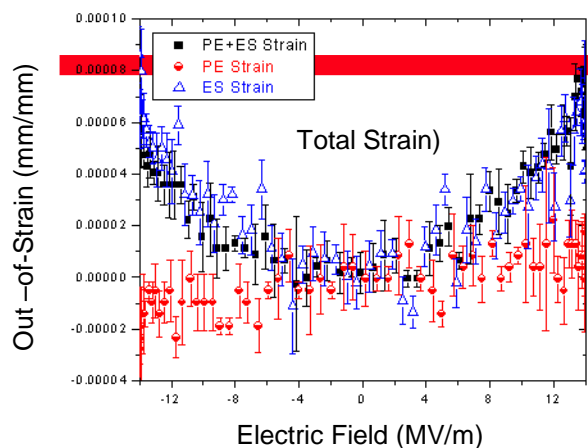


100 % Strain,
225°C slightly above T_g



Actuation of Unstretched/Stretched 2% BNNT/Polyimide

Unstretched

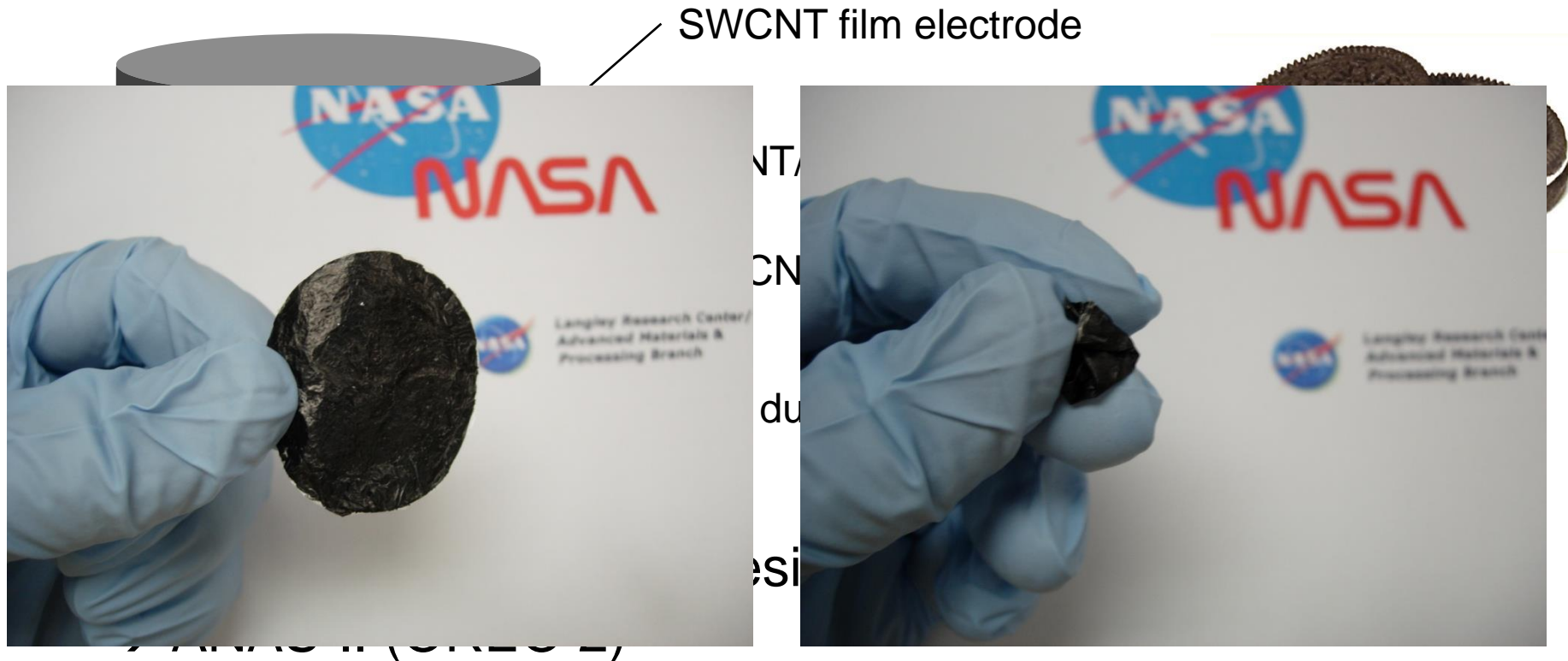


Origin of Actuation → BNNT

100% Stretched
@225°C, Quenching

100% Stretched
@225°C, Annealing

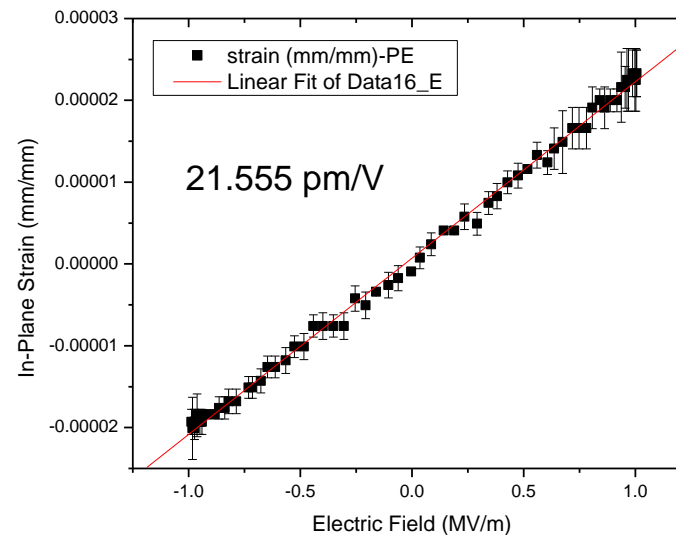
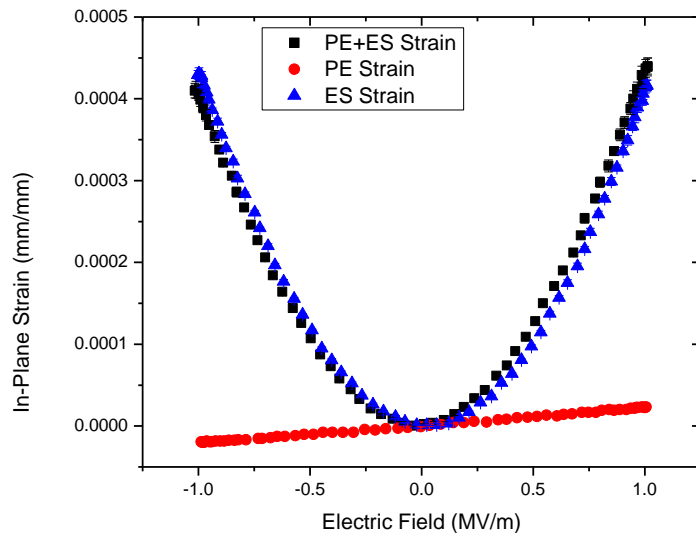
Langley All-Nanotubes Actuator/Sensor (LaRC-ANAS) Film



Goal: Flexible, transparent, large actuation, high sensitivity,
Mechanically Durable



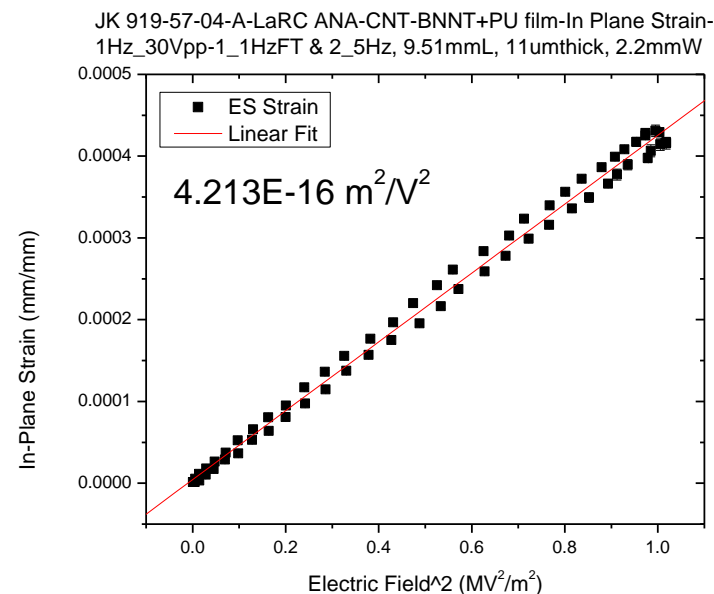
All-Nanotubes Actuator/Sensor Film: In-Plane Strain



Field induced strain (ϵ_{33})

$$\epsilon_{33} = d_{33} \cdot E + M_{33} \cdot E^2 + \dots$$

d_{33} : piezoelectric coefficient
 M_{33} : electrostrictive coefficient
 E : applied electric field





Actuation of Unstretched/Stretched h-BN/BNNT Materials

Materials	Inclusions	Polymer	Actuation
Polyimide (PI)	None	Polyimide	None
5%hBN/Polyimide (100% stretched)	5%hBN	Polyimide	None
5%BNNT (CVD)/Polyimide	5%BNNT (CVD)	Polyimide	None
Polyimide (100% stretched)	None	Polyimide	None
2%BNNT (laser)/Polyimide	2%BNNT	Polyimide	✓
2% BNNT (laser)/Polyimide (100% stretched)	2%BNNT	Polyimide	✓✓✓
20%BNNT/Polyurethane	>20% BNNT	Polyurethane	✓✓✓✓✓✓✓✓✓✓✓✓✓✓✓✓

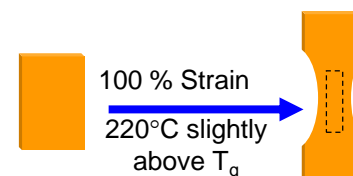
h-BN → No Actuation

Commercial BNNT (CVD) → No Actuation

Polymer → No Actuation

Stretched Polymer → No Actuation

BNNT (high pressure, high temp laser) → Origin of the Actuation





Radiation Shielding Properties

Modeling



Welcome to OLTARIS, the On-Line Tool for the Assessment of Radiation in Space. OLTARIS is an integrated tool set utilizing HZETRN (High Charge and Energy Transport). These tools are intended to help scientists and engineers study the effects of space radiation on shielding materials, electronics, and biological systems.

Science **340** 1080 (2013)

Measurements of Energetic Particle Radiation in Transit to Mars on the Mars Science Laboratory

C. Zeitlin,^{1*} D. M. Hassler,¹ F. A. Cucinotta,² B. Ehresmann,¹ R. F. Wimmer-Schweingruber,³ D. E. Brinza,⁴ S. Kang,⁴ G. Weigle,⁵ S. Böttcher,³ E. Böhm,³ S. Burmeister,³ J. Guo,² J. Köhler,³ C. Martin,³ A. Posner,⁶ S. Rafkin,¹ G. Reitz⁷

The Mars Science Laboratory spacecraft, containing the Curiosity rover, was launched to Mars on 26 November 2011, and for most of the 253-day, 560-million-kilometer cruise to Mars, the Radiation Assessment Detector made detailed measurements of the energetic particle radiation environment inside the spacecraft. These data provide insights into the radiation hazards that would be associated with a human mission to Mars. We report measurements of the radiation dose, dose equivalent, and linear energy transfer spectra. The dose equivalent for even the shortest round-trip with current propulsion systems and comparable shielding is found to be 0.66 ± 0.12 sievert.

Spacecraft data nails down radiation risk for humans going to Mars

Nature News, May 30, 2013, Ron Cowan

Interviewed Sheila Thibeault at NASA Langley about the study published in *Science*

Mars Science Laboratory (MSL) during its cruise to Mars between 6 December 2011 and 14 July 2012 (253 days)

Mars Round Trip Dose
Equivalent is around 0.66
Sievert

Image credit: NASA



Neutron Radiation Shielding Study

Materials

- Hydrogen, Boron, Nitrogen
- BN, BNNT, Gd
- Low density polyethylene (LDPE), polyimide (Kapton, CP2, (β -CN)APB/ODPA), polyurethane

Radiation Shielding Structural Materials

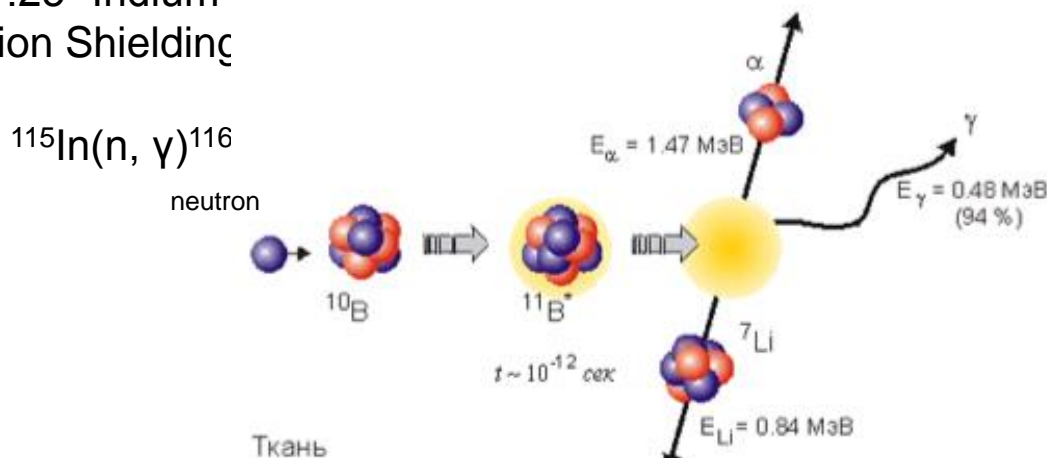
- In-situ polymerization under simultaneous sonication and shear
- Supercritical Fluid Infusion

Characterization

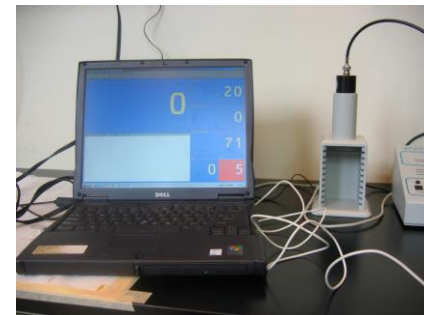
- Neutron Radiation Exposure Lab: Source: Am/Be 1Curie
- Moderated by borated polyethylene cylinder block (44mm thick):
45 mrem/hr thermal neutrons
- Sample: 2 x 2" polymer and BN polymer composites
- Detection Foil: 1.25" Indium Foil (0.5mm, 10 hours)
- RSMES: Radiation Shielding

Modeling

- OLTARIS



<http://www.inp.nsk.su/bnct/introduction/introduction.en.shtml>



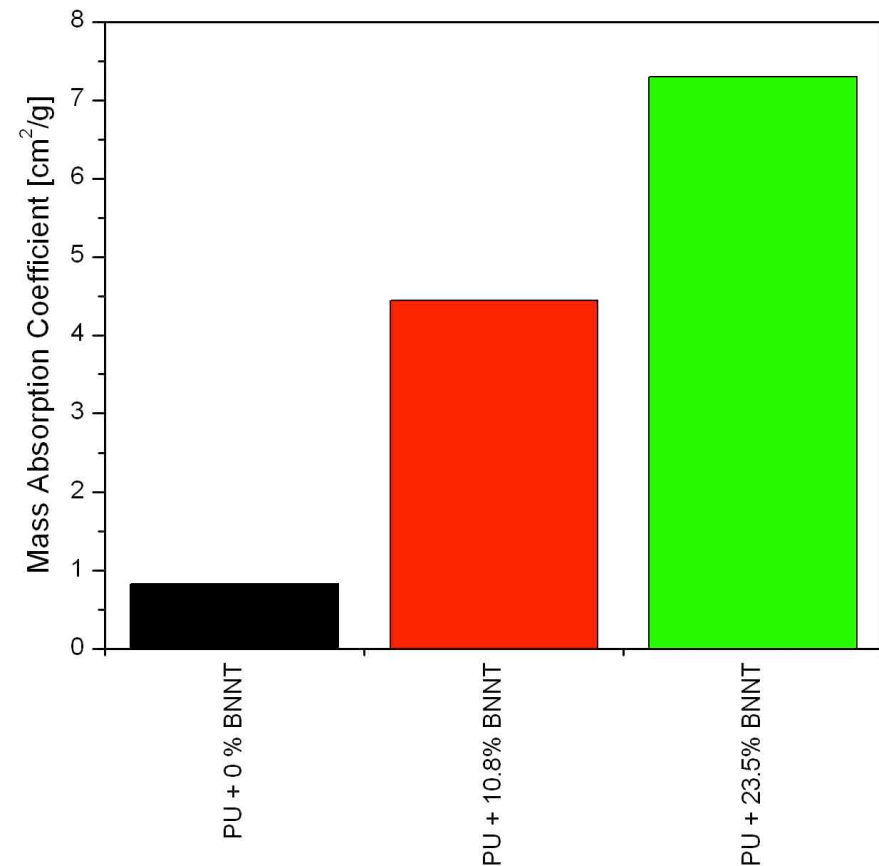
Geiger-Mueller Tube

All images credit: NASA



Advanced Radiation Shielding Materials Containing Hydrogen, Boron, and Nitrogen: Preliminary Results

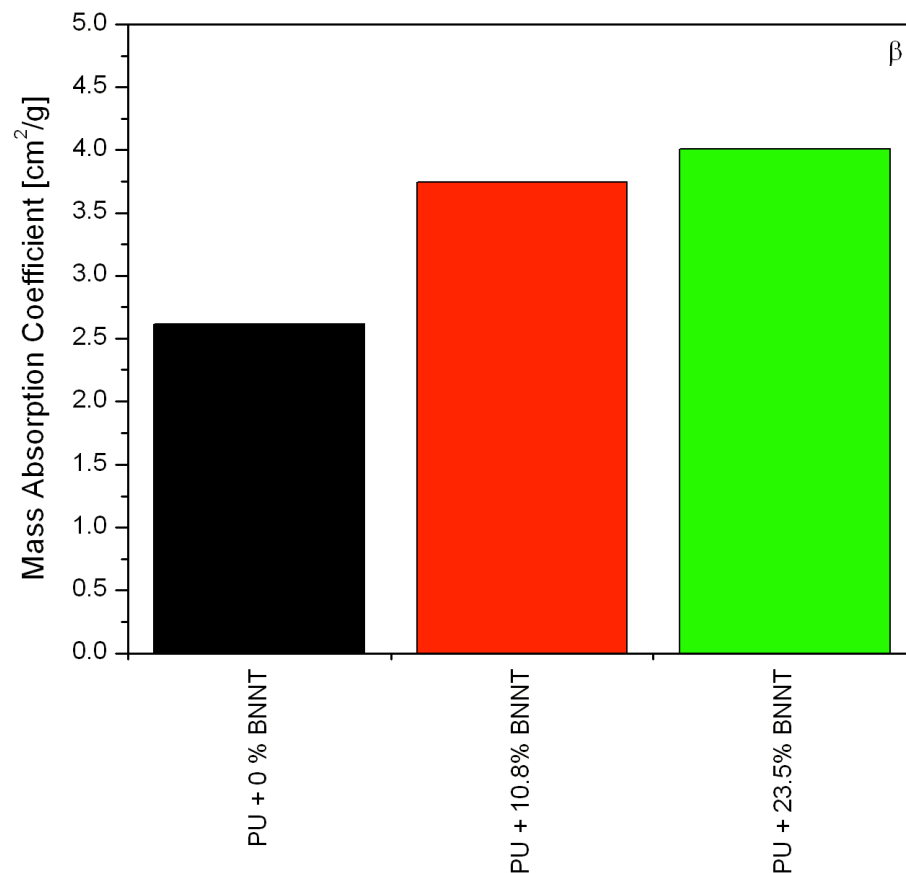
Neutron radiation



Am/Be 1Curie & moderated by borated PE



Beta radiation



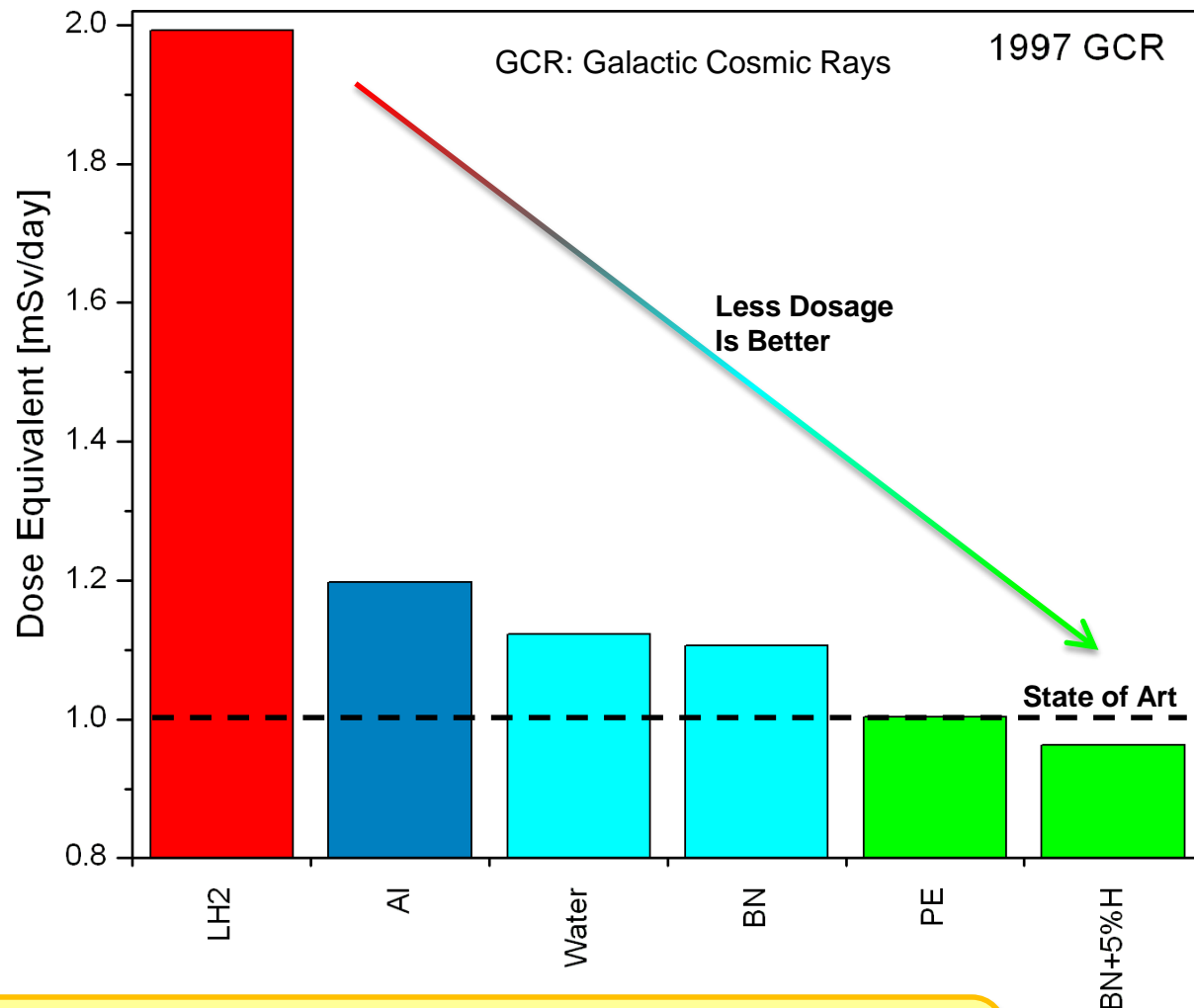
0.1 μCi Sr-90: β (Synthesized Apr 2009)





Dose Equivalent of Various Shielding Materials: OLTARIS Modeling: GCR 1997

Materials assumed to have common 30 cm thickness.



**BN materials perform better than LH2 and water.
BN+5%H performs better than state of art polyethylene.**



Summary

- $B_xC_yN_z$ Nanotubes (BNNT, BCNNT) were successfully synthesized with High Temperature-Pressure Laser Synthesis method.
- Development of multifunctional nanotube polymer nanocomposites with uniform dispersion.
- The Physical properties of nanocomposites can be tailored over a wide range by fine tuning the type of tubes, concentration, and degree of the alignment of nanotubes.
- In-situ diagnostics and modeling were implemented to support study of the BNNT and BCNNT nucleation and growth mechanism.
- Multifunctional Nanocomposites can sense strain, stress, pressure, damage, temperature.
- Multifunctional Nanocomposites can actuate through piezoelectrical and electrostrictive phenomena and generate large strain at low electric fields.
- Multifunctional Nanocomposites can shield radiation and high heat flux.



Thank You



All Images Credit: NASA